cells

MDPI

Article

Development of Innate-Immune-Cell-Based Immunotherapy for Adult T-Cell Leukemia–Lymphoma

Maho Nakashima [1,*], Yoshimasa Tanaka [2], Haruki Okamura [3], Takeharu Kato [4], Yoshitaka Imaizumi [5], Kazuhiro Nagai [6], Yasushi Miyazaki [7] and Hiroyuki Murota [1,8]

1 Department of Dermatology, Graduate School of Biomedical Sciences, Nagasaki University, Nagasaki 852-8501, Japan
2 Center for Medical Innovation, Nagasaki University, Nagasaki 852-8588, Japan; ystanaka@nagasaki-u.ac.jp
3 Department of Tumor Cell Therapy, Hyogo College of Medicine, Nishinomiya 663-8501, Japan; haruoka6261274@gmail.com
4 Department of Hematology, Nagasaki University Hospital, Nagasaki 852-8501, Japan
5 Department of Hematology, National Hospital Organization Nagasaki Medical Center, Omura 856-8562, Japan
6 Department of Clinical Laboratory, National Hospital Organization Nagasaki Medical Center, Omura 856-8562, Japan; nagai.kazuhiro.zp@mail.hosp.go.jp
7 Department of Hematology, Atomic Bomb Disease Institute, Nagasaki University, Nagasaki 852-8523, Japan
8 Leading Medical Research Core Unit, Life Science Innovation, Nagasaki University Graduate School of Biomedical Sciences, Nagasaki 852-8521, Japan
* Correspondence: mahoko19870319@gmail.com; Tel.: +81-95-819-7333

Abstract: γδ T cells and natural killer (NK) cells have attracted much attention as promising effector cell subsets for adoptive transfer for use in the treatment of malignant and infectious diseases, because they exhibit potent cytotoxic activity against a variety of malignant tumors, as well as virus-infected cells, in a major histocompatibility complex (MHC)-unrestricted manner. In addition, γδ T cells and NK cells express a high level of CD16, a receptor required for antibody-dependent cellular cytotoxicity. Adult T-cell leukemia–lymphoma (ATL) is caused by human T-lymphotropic virus type I (HTLV-1) and is characterized by the proliferation of malignant peripheral $CD4^+$ T cells. Although several treatments, such as chemotherapy, monoclonal antibodies, and allogeneic hematopoietic stem cell transplantation, are currently available, their efficacy is limited. In order to develop alternative therapeutic modalities, we considered the possibility of infusion therapy harnessing γδ T cells and NK cells expanded using a novel nitrogen-containing bisphosphonate prodrug (PTA) and interleukin (IL)-2/IL-18, and we examined the efficacy of the cell-based therapy for ATL in vitro. Peripheral blood samples were collected from 55 patients with ATL and peripheral blood mononuclear cells (PBMCs) were stimulated with PTA and IL-2/IL-18 for 11 days to expand γδ T cells and NK cells. To expand NK cells alone, $CD3^+$ T-cell-depleted PBMCs were cultured with IL-2/IL-18 for 10 days. Subsequently, the expanded cells were examined for cytotoxicity against ATL cell lines in vitro. The proportion of γδ T cells in PBMCs was markedly low in elderly ATL patients. The median expansion rate of the γδ T cells was 1998-fold, and it was 12-fold for the NK cells, indicating that γδ T cells derived from ATL patients were efficiently expanded ex vivo, irrespective of aging and HTLV-1 infection status. Anti-CCR4 antibodies enhanced the cytotoxic activity of the γδ T cells and NK cells against HTLV-1-infected CCR4-expressing $CD4^+$ T cells in an antibody concentration-dependent manner. Taken together, the adoptive transfer of γδ T cells and NK cells expanded with PTA/IL-2/IL-18 is a promising alternative therapy for ATL.

Keywords: adult T-cell leukemia–lymphoma; γδ T cell; infusion therapy; interleukin-2; interleukin-18; nitrogen-containing bisphosphonate prodrug; NK cell

Citation: Nakashima, M.; Tanaka, Y.; Okamura, H.; Kato, T.; Imaizumi, Y.; Nagai, K.; Miyazaki, Y.; Murota, H. Development of Innate-Immune-Cell-Based Immunotherapy for Adult T-Cell Leukemia–Lymphoma. *Cells* **2024**, *13*, 128. https://doi.org/10.3390/cells13020128

Academic Editor: Subramaniam Malarkannan

Received: 21 November 2023
Revised: 31 December 2023
Accepted: 6 January 2024
Published: 10 January 2024

1. Introduction

Adult T-cell leukemia–lymphoma (ATL) is a mature peripheral $CD4^+$ T-cell malignancy caused by infection with human T-lymphotropic virus type I (HTLV-1) [1]. ATL was first discovered in Japan, in 1977 [1,2]. HTLV-1 infections are endemic in some countries and regions, including Japan, Latin America, southwestern Africa, and some areas of Australia [3]. In Japan, there are more than one million carriers of HTLV-1 [4]; 4000 new cases of HTLV-1 infection per year [5]; approximately 2600 cases of newly diagnosed ATL within a 2 y period [6]; and 1000–1500 deaths from ATL annually [7]. ATL is usually categorized into four subtypes based on clinical findings: acute, lymphoma, chronic, and smoldering [8,9]. This classification is useful for making decisions concerning treatment. According to the criteria used to diagnose ATL [8], the indolent subtypes (i.e., smoldering and favorable chronic) are usually managed with watchful waiting until acute crisis [10], and the aggressive subtypes (i.e., acute, lymphoma, and unfavorable chronic) are managed using a variety of intensive chemotherapies followed by allogeneic hematopoietic stem cell transplantation (allo-HSCT) depending on the age [11,12]. More recently, anti-CC chemokine receptor 4 (CCR4) monoclonal antibody (mAb) (mogamulizumab) [13,14] and lenalidomide [15] have also been used for treating relapsed or refractory ATL. However, ATL generally exhibits a very poor prognosis. In fact, the recent 4-year survival rates (i.e., the median survival time, days) for acute-, lymphoma-, unfavorable chronic-, favorable chronic-, and smoldering-subtype ATL in Japan were 16.8% (252), 19.6% (305), 26.6% (572), 62.1% (1937), and 59.8% (1851), respectively [16]. Moreover, the 3-year overall survival rate for acute- or lymphoma-subtype ATL was reported to be 33% despite undergoing allo-HSCT, which is considered to be the only curative treatment, but which frequently causes severe adverse events [17]. It is, therefore, imperative to develop novel modalities for the treatment of ATL.

In Japan, the median age at diagnosis of ATL is 68 years old (interquartile range: 60–75 years old) [18]. In general, ATL onset requires a long latency period of approximately 50–60 years, which indicates the involvement of multistep mechanisms for leukemogenesis in HTLV-1-infected cells. The HTLV-1 proteins Tax and HBZ are involved in the alteration of immune traits in HTLV-1-infected cells, escape from host immune surveillance systems, and accumulation of genetic mutations [19–23]. It was reported that the frequencies of invariant natural killer T (iNKT) cells, NK cells, and dendritic cells in the peripheral blood of ATL patients were significantly decreased [24] and that NK cell activity was markedly low in ATL patients [25]. Recently, the adoptive transfer of autologous NK cells was reported to be effective and safe [26–30]. Immunotherapy is, therefore, considered to be a novel therapeutic and prophylactic strategy against HTLV-1 infections.

The adoptive transfer of T cells and NK cells has attracted much attention as a new strategy for cancer immunotherapy. Chimeric antigen receptor (CAR) T-cell therapy is a revolutionary new pillar in the treatment of B-cell lymphoma and multiple myeloma [31,32]. There are, however, many problems related to CAR T-cell therapy, such as life-threatening CAR T-cell-associated toxicities, limited efficacy against solid tumors, inhibition and resistance in B-cell malignancies, antigen escape, limited persistence, poor trafficking and tumor infiltration, and the immunosuppressive microenvironment [33]. With CAR NK cells, it is generally difficult to expand a large number of highly active NK cells for infusion therapies [26,29].

The aims of this study were to develop an efficient method for expanding autologous innate immune effector cells and to confirm whether the expanded cells exhibit potent cytotoxic activities against HTLV-1-infected cells in vitro. We focused on γδ T cells and NK cells as innate immune effector cells and examined the expansion rate and cytotoxicity against HTLV-1-infected cells.

γδ T cells are involved in an immune surveillance system against cancer, including hematological diseases and solid tumors [34–45]. γδ T cells occupy 3–5% of peripheral blood T cells, 50–75% of which express Vγ9 (also termed Vγ2)- and Vδ2-bearing T-cell receptors (TCRs) in healthy adults [46]. We hereafter use the term "γδ T cells" for Vγ9–Vδ2-

bearing γδ T cells. Most γδ T cells express neither CD4 nor CD8 and do not require conventional antigen processing and presentation via major histocompatibility complex (MHC) molecules for antigen recognition. In addition, the majority of γδ T cells fail to recognize conventional peptide antigens. Instead, they recognize small phosphorylated metabolites, such as isopentenyl diphosphate (IPP) and dimethylallyl diphosphate (DMAPP), from the mevalonate pathway, as self-antigens and (*E*)-4-hydroxy-3-methylbut-2-enyl diphosphate (HMBPP) from the 2-*C*-methyl-D-erythritol 4-phosphate/1-deoxy-D-xylulose 5-phosphate (MEP/DOXP) pathway as a foreign antigen in a butyrophilin (BTN) 3A1/2A1-dependent manner [47,48]. Since the multifaceted properties of tumor cells depend on the spaciotemporal expressions of small G-proteins, such as Ras, Rap, and Rho, whose functions are inexorably linked to farnesyl and/or geranylgeranyl-groups derived from metabolites in the mevalonate pathway, tumor cells might contain an elevated level of IPP/DMAPP, which can be recognized by γδ T cells [49].

γδ T cells derived from the peripheral blood of young, healthy donors (hereafter referred to as HDs) can be efficiently expanded up to 95–99% for 10–11 days with tetrakis-pivaloyloxymethyl 2-(thiazole-2-ylamino) ethylidene-1,1-bisphosphonate (PTA), a nitrogen-containing bisphosphonate prodrug, and interleukin (IL)-2 [50]. Although IL-2 can expand NK cells, the extent is not sufficient for practical use in clinical settings. The IL-18 receptor is expressed on innate immune cells, such as γδ T cells and NK cells, and IL-18 could augment the proliferation of γδ T cells and promote the expansion of NK cells in the presence of IL-2, since IL-18 induces the expression of CD25, an IL-2 receptor α chain [51–53].

It is worth noting that a humanized anti-CCR4 mAb has been approved for the treatment of ATL, in which the mAb acts on CCR4-expressing HTLV-1-infected $CD4^+$ T cells [54–56]. The therapeutic effect of anti-CCR4 mAb is considered to be partially dependent on antibody-dependent cellular cytotoxicity (ADCC) through FcγR IIIa (CD16) expressed on effector cells, such as γδ T cells and NK cells [51,55,57–59]. It is, therefore, intriguing to examine whether anti-CCR4 mAb enhances the cytotoxicity of γδ T cells and NK cells against HTLV-1-infected cells in vitro.

Since γδ T cells and NK cells are not restricted by MHC in the recognition of malignant cells, the allogeneic transfer of these innate immune cells is currently under investigation. It is, however, evident that autologous cell therapies are safer than allogeneic cell therapies, since residual αβ T cells might cause graft-versus-host diseases.

In this study, we examined the immunological properties of γδ T cells and NK cells derived from HDs, elderly non-ATL patients and ATL patients in an attempt to explore the possibility of the adoptive transfer of γδ T cells and NK cells in the treatment of ATL.

2. Materials and Methods

2.1. Derivation of γδ T Cells and NK Cells

γδ T cells were expanded from peripheral blood mononuclear cells (PBMCs) in Yssel's medium supplemented with 10% heat-inactivated human AB serum [60], as described in Supplementary Figure S1. NK cells were prepared from CD3-depleted PBMC, as described in Supplementary Figure S2.

2.2. Flow Cytometric Analysis

Cells were stained with fluorescent dye-conjugated Abs, as described in Supplementary Figures S1–S7, and analyzed using a FACS Lyric flow cytometer (Becton Dickenson, Franklin, Lakes, NJ, USA). The cell population was visualized with FlowJo ver. 10.8.1 (FlowJo LLC, Ashland, OR, USA).

2.3. Patient Characterization and Outcome

This study was conducted in accordance with the Declaration of Helsinki and was approved by the Institutional Review Board of Nagasaki University Hospital. Obligatory written informed consent was obtained from each participant in accordance with the

comprehensive prior consent given to the Departments of Hematology and Dermatology (Approval No. 13022512 and UMIN000042835).

In this study, 16 HDs with no known medical history (12 males and 4 females) were first enrolled. The median age at the time of blood sampling was 34 years (range: 27–58 years). γδ T cells and/or NK cells were expanded from the peripheral blood samples of 10 HDs, as shown in Supplementary Table S1. Then, 55 ATL patients were recruited in this study. Patients' characteristics are summarized in Supplementary Table S2 and the Shimoyama classification at the first diagnosis and the outcome at blood sampling are summarized in Supplementary Table S3. ATL patients were allocated to flow cytometric analysis, PTA/IL-2-induced expansion of γδ T cells, PTA/IL-2/IL-18-induced expansion of γδ T cells, and IL-2/IL-18-induced expansion of NK cells, which is summarized in Supplementary Table S4. In addition, elderly non-ATL patients (8 males and 2 females) were enrolled, as shown in Supplementary Table S5, since aging is reported to result in the remodeling of T-cell immunity and to be associated with poor clinical outcomes in age-related diseases [61]. They visited the Department of Dermatology, Nagasaki University Hospital between December 2021 and July 2023 and had no history of malignancy, HTLV-1 infections, and use of immunosuppressants or prednisolones. The median age at the time of blood sample collection was 71.5 years old (range: 66–92 years old), which is comparable to that of the ATL patients.

2.4. Cytotoxicity Assay Using Time-Resolved Fluorescence Spectroscopy

The cytotoxic activity of γδ T cells and NK cells against HTLV-1-infected cells was determined using a nonradioactive cellular cytotoxicity assay kit (Techno Suzuta Co., Ltd., Heiwa-machi, Nagasaki, Japan). The KK1 human ATL cell line was established in the Department of Hematology, Nagasaki University, and the HuT102 human ATL cell line was from American Type Culture Collection (ATCC, Manassas, VA, USA). The cell lines were maintained in complete RPMI1640 medium at 37 °C with 5% CO_2 overnight. As for the ATL cell lines, 100 U/mL of IL-2 was added to the medium every other day. KK1 and HuT102 were pretreated with anti-CCR4 mAb (Kyowa Kirin Co., Ltd., Chiyoda-ku, Tokyo, Japan) (4 mg/mL stock solution in PBS) at final concentrations of 0.5 μg/mL and 10 μg/mL, respectively. The tumor cell suspensions (1×10^6 cells in 1 mL of RPMI1640 medium) were then pulsed with 25 μM bis (butyryloxymethyl) 4′-(hydroxymethyl)-2,2′:6′,2″-terpyridine-6,6′-dicarboxylate (BM-HT, Techno Suzuta Co., Ltd.) at 37 °C for 15 min. When BM-HT was internalized in the tumor cells, the compound was hydrolyzed by intracellular esterases to yield 4′-(hydroxymethyl)-2,2′:6′,2″-terpyridine-6,6″-dicarboxylate (HT). Afterward, the cells were washed three times with 5 mL of complete RPMI1640 via centrifugation at 1700 rpm at 4 °C for 5 min. The tumor cell suspensions (5×10^3 cells/100 μL) were dispensed into a 96-well round-bottom plate, to which was added 100 μL of a serial dilution of γδ T cells and/or NK cells. The plate was briefly centrifuged at 500 rpm at room temperature for 2 min and then incubated at 37 °C with 5% CO_2 for 60 min. Detergent (Techno Suzuta Co., Ltd.) was added to each well at a final concentration of 5×10^{-5} M for maximum release, and the cell suspensions and the plate were incubated at 37 °C with 5% CO_2 for 20 more min. After the cell suspensions were mixed well, the plate was centrifuged at 1700 rpm at 4 °C for 2 min. The supernatant, 25 μL each, was transferred to a new 96-well round-bottom plate containing 250 μL of europium (Eu^{3+}) solution in 0.3 M sodium acetate buffer at pH 4 (Techno Suzuta Co., Ltd.), from which 200 μL each was transferred to Thermo Scientific 96-well plates. The time-resolved fluorescence (TRF) was measured using a NIVO multiplate reader (Revvity, Yokohama, Kanagawa, Japan). All measurements were performed in triplicate. The specific lysis (%) was calculated as 100 × (experimental release (counts) − spontaneous release (counts))/(maximum release (counts) − spontaneous release (counts)).

2.5. Statistical Analysis

Continuous data are presented as the median value, range, and interquartile range (IQR), and they were compared using Wilcoxon rank-sum tests with GraphPad Prism (version 10.0.2 for Windows, GraphPad Software, La Jolla, CA, USA). Categorical data were compared using Fisher's exact tests. A *p*-value of less than 0.05 was considered to be statistically significant.

3. Results

3.1. Expansion of γδ T Cells and NK Cells Derived from HDs

We first expanded γδ T cells from PBMC of 10 HDs using PTA/IL-2, as shown in Supplementary Table S1. Four representative results of the flow cytometric analyses before and after expansion are shown in Supplementary Figure S1A. It is of note that a large number of highly purified γδ T cells were obtained by using a PTA/IL-2 expansion system [50], when the initial proportion of γδ T cells in the $CD3^+$ lymphocyte fractions was well above 1%. The stimulated cells started to form clusters 3 to 5 days following the stimulation (Supplementary Figure S1B). NK cell-related cell surface markers [62–67], such as natural killer group 2 member D (NKG2D), DNAX accessory molecule-1 (DNAM-1), and CD16 (FcγRIIIA), were expressed on γδ T cells on day 11 (Supplementary Figure S1C). By contrast, the expression of FasL (CD95L) and TRAIL (human TNF-related apoptosis-inducing ligand) was marginal. PD-1 was expressed on γδ T cells to different degrees depending on individuals, which was consistent with previous reports [68,69].

We next expanded NK cells using IL-2 and IL-18 from 10 HDs. As shown in Supplementary Figure S2A, highly purified NK cells were obtained on day 10. The stimulated cells started to form clusters 4 to 5 days after stimulation with IL-2/IL-18 (Supplementary Figure S2B). The NK cells expanded for 10 days expressed high levels of NKG2D, DNAM-1, and CD16, as shown in Supplementary Figure S2C. In addition, more than half of the IL-2/IL-18-expanded NK cells expressed high levels of HLA-DQ [70] and CD86 [71].

3.2. Cytotoxicity Exhibited by γδ T Cells and NK Cells Derived from HDs against ATL Cell Lines In Vitro

We next examined the cytotoxic activity exhibited by PTA/IL-2-expanded γδ T cells against HTLV-1-infected cell lines with a time-resolved fluorescence (TRF)-based assay system using a terpyridine derivative and europium [72]. We examined the effect of anti-CCR4 mAb on the γδ T-cell-mediated cytotoxicity against KK1 and HuT102 HTLV-1-infected cell lines. As shown in Figure 1 (left panels), the γδ T cells exhibited potent cytotoxic activity against KK1 and HuT102 cells in an E/T ratio-dependent manner, with the specific lysis reaching approximately 20% in 60 min at an E/T ratio of 1:200. When 10 μg/mL of anti-CCR4 mAb was added to the assay system, 40 to 80% of either KK1 or HuT102 cells were killed by γδ T cells at an E/T ratio of 1:100, suggesting that the γδ T cells exhibited a potent ADCC against HTLV-1-infected cells in the presence of anti-CCR4 mAb (Figure 1, middle and right panels).

Following this, we examined the direct cellular cytotoxicity of the NK cells against HTLV-1-infected cells. As shown in Figure 2 (left panels), the specific lysis of NK cells against KK1 or HuT102 reached 20% to 70% in 60 min at an E/T ratio of 1:100. It is worth noting that the NK cells exhibited a more potent cellular cytotoxicity against HTLV-1-infected cells than the γδ T cells. When 10 μg/mL of anti-CCR4 mAb was added to the assay system, more than 40–80% of KK1 and HuT102 cells were killed by NK cells at an E/T ration of 1:100. Taken together, innate immune cells, including γδ T cells and NK cells derived from HDs, exhibited both a direct cellular cytotoxicity and ADCC against HTLV-1-infected cells.

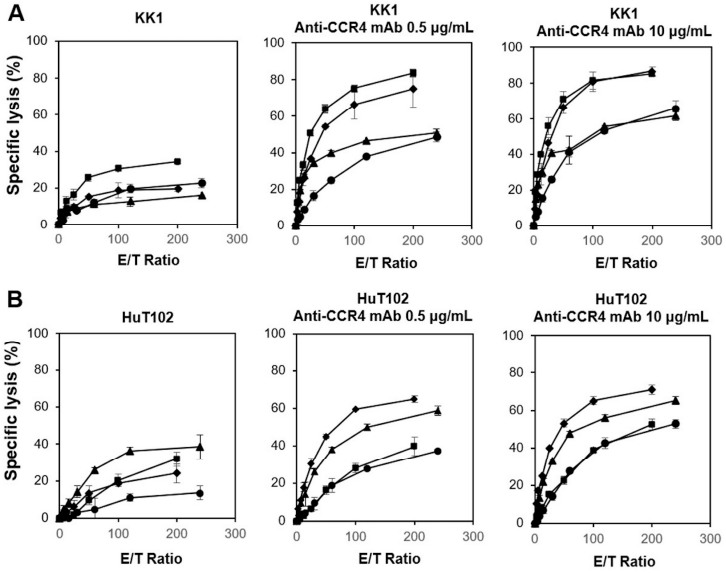

Figure 1. Cytotoxic activity exhibited by γδ T cells derived from HDs against HTLV-1-infected cells. Effect of anti-CCR4 mAb on the cytotoxic activity of γδ T cells against KK1 (**A**) and HuT102 (**B**). After HTLV-1-infected cell lines were pretreated with 0, 0.5, or 10 μg/mL of anti-CCR4 mAb for 15 min, the sensitized cells were challenged with PTA/IL-2-stimulated/expanded γδ T cells derived from four HDs at E/T ratios of 3.90625:1, 7.8125:1, 15.625:1, 31.25:1, 62.5:1, 125:1, and 250:1 or 3.125:1, 6.25:1, 12.5:1, 25:1, 50:1, 100:1, and 200:1 for 60 min, and the specific lysis was determined using a time-resolved fluorescence-based assay based on an europium–terpyridine derivative chelate. The various symbols depict the cytotoxic activity of γδ T cells from distinct HDs.

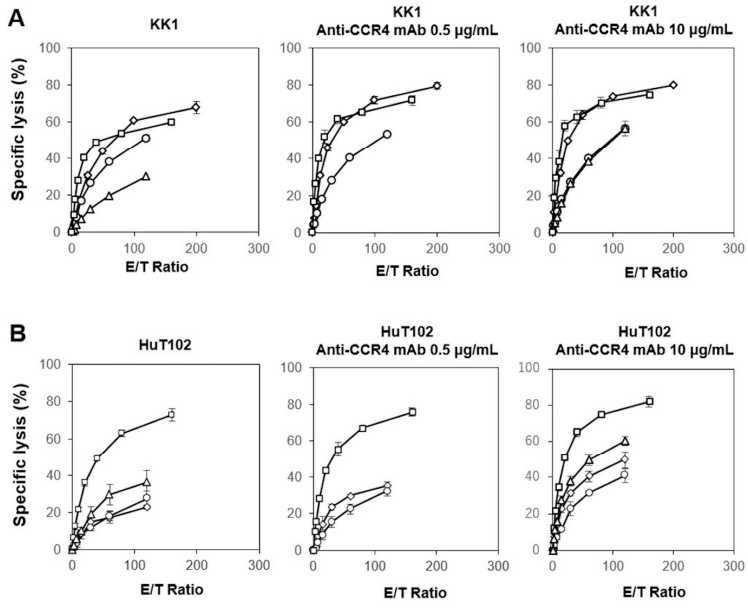

Figure 2. Cytotoxic activity exhibited by NK cells derived from HDs against HTLV-1-infected cells. Effect of anti-CCR4 mAb on the cytotoxic activity of NK cells against KK1 (**A**) and HuT102 (**B**). After HTLV-1-infected cell lines were pretreated with 0, 0.5, or 10 μg/mL of anti-CCR4 mAb for 15 min, the sensitized cells were challenged with PTA/IL-2-stimulated/expanded γδ T cells derived from four HDs at E/T ratios of 2.5:1, 5:1, 10:1, 20:1, 40:1, 80:1, and 160:1 or 1.875:1, 3.75:1, 7.5:1, 15:1, 30:1, 60:1, and 120:1 for 60 min, and the specific lysis was determined using a time-resolved fluorescence-based assay based on an europium–terpyridine derivative chelate. The various symbols depict the cytotoxic activity of γδ T cells from distinct HDs.

3.3. Effect of IL-18 on the Expansion of γδ T Cells Derived from ATL Patients

We then examined the immunological properties of γδ T cells derived from ATL patients. The frequency of Vδ2$^+$ T cells in CD3$^+$ T cells was significantly low in the peripheral blood of 25 ATL patients compared to that of HDs, as shown in Figure 3A. When PBMCs derived from ATL patients were stimulated/expanded with PTA/IL-2 for 11 days, the γδ T cells proliferated well and the expansion rate was comparable to that of HDs, as shown in Figure 3B, which indicates that the PTA/IL-2-mediated expansion of the γδ T cells was not affected by age and HTLV-1 infection status in terms of the expansion rate.

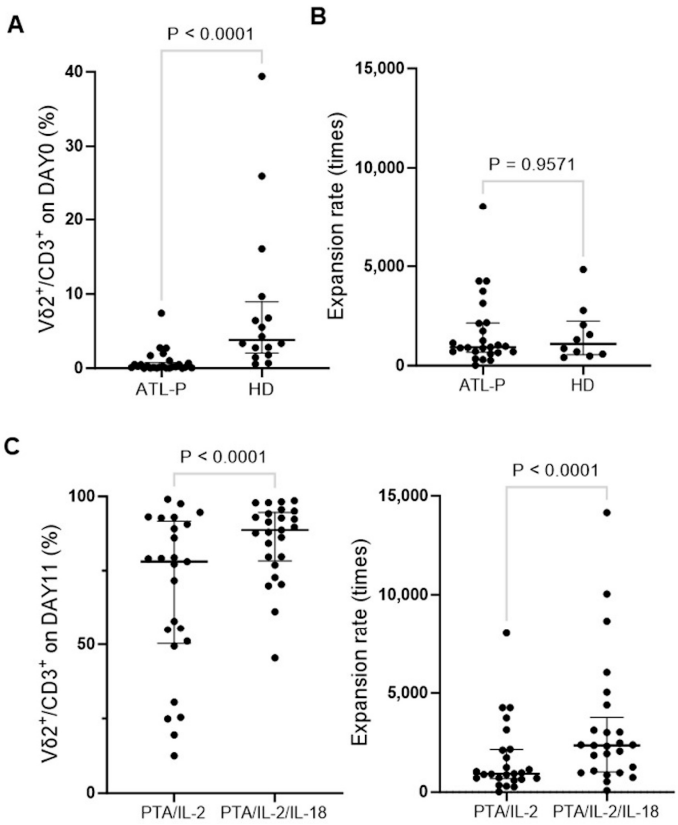

Figure 3. Comparison of the γδ T-cell expansions between ATL patients and HDs. (**A**) Proportion of γδ T cells in CD3$^+$ T cells before expansion. PBMCs from 25 ATL patients and 10 HDs were purified from peripheral blood samples and stained with PE-conjugated anti-CD3 mAb and FITC-conjugated anti-Vδ2 mAb, which were analyzed using a FACS Lyric flow cytometer. (**B**) Expansion rate of γδ T cells in response to PTA/IL-2. After stimulation/expansion with PTA/IL-2 for 11 days, the cells were stained and analyzed as in (**A**) and counted under a microscope to calculate the number of γδ T cells. (**C**) Comparison of PTA/IL-2 and PTA/IL-2/IL-18 in the expansion of γδ T cells. PBMCs were stimulated/expanded with either PTA/IL-2 or PTA/IL-2/IL-18, and the effect of IL-18 was examined using flow cytometric analyses and the cell counting method.

In the studies on γδ T cells derived from HDs, it was difficult to obtain a large number of highly purified γδ T cells when the initial proportion of γδ T cells in the CD3$^+$ lymphocyte fractions was too low, especially when the proportion was less than 1%. In the peripheral blood of ATL patients, in fact, the initial frequency of γδ T cells was mostly less than 1%. We therefore sought to develop a strategy to expand γδ T cells more efficiently even in the case of ATL patients whose proportion of peripheral blood γδ T cells was markedly low.

It was previously demonstrated that the IL-18 receptor is expressed on immune effector cells, such as NK cells, γδ T cells, and CD8$^+$ killer T cells, and IL-18 could efficiently promote the expansion of γδ T cells [52] and NK cells [53] with potent cytotoxicity. We therefore expanded PBMCs derived from the same 25 ATL patients with PTA/IL-2/IL-18 for 11 days

(under the same conditions, except for the addition of IL-18) and examined the proportion of γδ T cells in $CD3^+$ T cells. As shown in Figure 3C, PTA/IL-2/IL-18 successfully amplified γδ T cells derived from 25 ATL patients, and the purity of the γδ T cells was higher than that for those expanded with PTA/IL-2. In addition, the expansion rate of the γδ T cells stimulated with PTA/IL-2/IL-18 was also greater than that for PTA/IL-2. We therefore enrolled 30 additional ATL patients and analyzed the PTA/IL-2/IL-18-mediated expansion of γδ T cells derived from a total of 55 ATL patients.

As shown in Supplementary Figure S3A, the initial proportion of γδ T cells was markedly low, compared to that of HDs. It is worthy of note that some $CD4^+$ T cells expressed a slightly low level of CD3. It is most likely that the $CD3^{dim}CD4^+$ T cell population corresponds to ATL cells. A microscopic analysis revealed that the cells started to form clusters 3 to 6 days after stimulation depending on individuals (Supplementary Figure S3B). After expansion with PTA/IL-2/IL-18 for 11 days, the proportion of γδ T cells in lymphocyte fractions failed to reach to the levels for HDs, whereas the expansion rate was equivalent to that for HDs. It is intriguing that $CD3^{dim}CD4^+$ T cells mostly disappeared from the cell culture, suggesting that they were killed by γδ T cells. In fact, essentially all the expanded γδ T cells expressed NKG2D and DNAM-1, as shown in Supplementary Figure S3C. They expressed CD16 and PD-1 to different degrees depending on individuals. In addition, it is noteworthy that $CD3^-CD56^+$ cells were increased when the proportion of γδ T cells was low on day 11. It is most likely that this $CD3^-CD56^+$ cell population is NK cells, indicating that the ATL cells in the cell culture are also killed by NK cells.

Based on the above findings, it is essential to take the initial proportion of γδ T cells and the expansion of NK cells into account when we further explore the possibility of infusion therapy for ATL. As shown in Supplementary Figure S4, $CD3^-CD56^+$ cells (corresponding to NK cells) were increased when γδ T cells failed to occupy the majority of lymphocytes after stimulation/expansion with PTA/IL-2/IL-18 for 11 days. Even in such cases, $CD3^{dim}CD4^+$ T cells (corresponding to ATL cells) disappeared after incubation for 11 days, strongly suggesting that PTA/IL-2/IL-18-expanded γδ T cells and NK cells could exert potent anti-ATL activity.

Hence, the ATL patients were divided into two groups: one that exhibited an initial frequency of γδ T cells in $CD3^+$ T cells of less than 0.1% and one that was 0.1% or greater. In the group with a γδ T-cell frequency of less than 0.1%, the purity of the γδ T cells after expansion with PTA/IL-2/IL-18 for 11 days was significantly lower than that for the other group, as shown in Figure 4A. It is worth noting that the group with a lower proportion of γδ T cells tended to have a worse disease status, as determined using clinical indicators such as sIL-2R (U/mL), LDH (IU/L), BUN (mg/dL), WBCs ($\times 10^9$/L), and Ab-Ly (%) (Figure 4B). Using Fisher's exact tests, the low-frequency group had significantly more aggressive diagnoses (i.e., acute, lymphoma, and unfavorable chronic subtypes) based on the Shimoyama classification at the time of blood sampling (10 out of the 16 patients in this group, $p = 0.0324$), demonstrating that ATL patients with an aggressive-type diagnosis according to the Shimoyama classification tended to exhibit poor expansion of γδ T cells with PTA/IL-2/IL-18. In most cases, NK cells were expanded instead of γδ T cells after incubation with PTA/IL-2/IL-18. In three ATL patients who did not respond to PTA/IL-2/IL-18 at all, Ab-Ly occupied more than 90% of WBCs before expansion, and more than 90% of the cells remained ATL cells after expansion. However, such a poor expansion of γδ T cells and NK cells was observed in only a small number of the ATL patients, indicating that the development of infusion therapy using autologous γδ T cells and NK cells is feasible with most of the ATL patients.

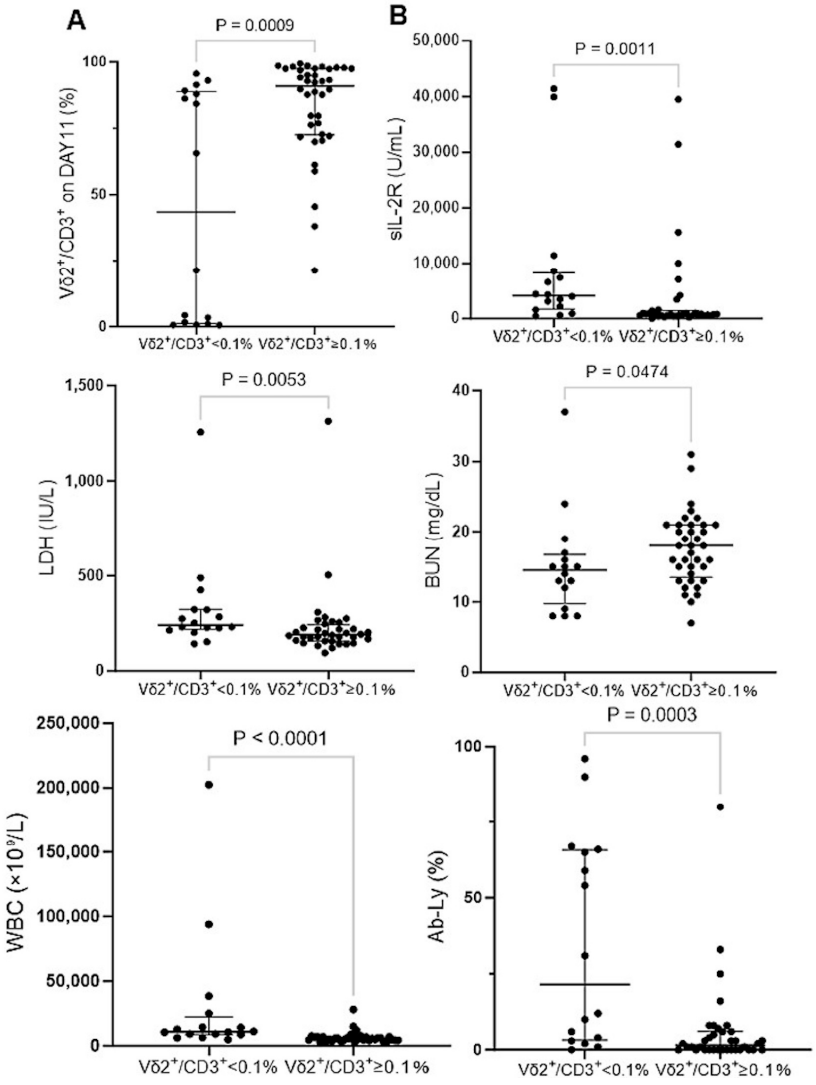

Figure 4. Effect of the initial proportion of Vδ2$^+$ T cells in CD3 cells on the expansion of γδ T cells and comparison of blood test results between ATL patients with relatively high levels of initial Vδ2/CD3 ratio (greater than 0.1%) and those with low levels (less than 0.1%). (**A**) Proportion of Vδ2$^+$ cells in CD3 cells after expansion of PBMCs with PTA/IL-2/IL-18. After stimulation/expansion of PBMCs derived from ATL patients with PTA/IL-2/IL-18, the cells were analyzed through a FACS Lyric flow cytometer. (**B**) Comparison of blood test results stratified by the initial proportion of Vδ2$^+$ T cells in CD3 cells. Laboratory test results were compared based on the initial proportion of Vδ2$^+$ T cells in CD3$^+$ T cells.

3.4. IL-2/IL-18-Mediated Expansion of NK Cells Derived from ATL Patients

Since NK cells derived from HDs exhibited a potent cellular cytotoxicity against ATL cells and NK cells were expanded in the culture of ATL patient-derived PBMCs with a low proportion of γδ T cells in the presence of PTA/IL-2/IL-18, we set out to examine the effector functions of IL-2/IL-18-stimulated/expanded NK cells derived from 30 ATL patients. However, two particular cases with high Ab-Ly counts and extremely low CD3$^-$ T lymphocyte counts were excluded from analysis.

As shown in Supplementary Figure S5, the proportion of NK cells derived from ATL patients after expansion with IL-2/IL-18 for 10 days was comparable to that from HDs, whereas the expansion rate was significantly lower than that of HDs. The expression of NKG2D, DNAM-1, CD16, HLA-DQ, and CD86 in NK cells derived from ATL patients after expansion was equivalent to that of HDs.

3.5. Effect of Aging on the Phenotype and Immunological Properties of γδ T Cells and NK Cells

Since most ATL patients are elderly, it is essential to examine the effect of aging on the phenotype and immunological properties of γδ T cells and NK cells to distinguish the effect of the HTLV-1 infection status and age. We obtained peripheral blood samples from 10 elderly non-ATL patients, whose median age was comparable to that of ATL patients. After PBMCs were stimulated/expanded with PTA/IL-2/IL18 (see Supplementary Note added to Result Section 3.5), we compared cell surface markers on γδ T cells before and after expansion with PTA/IL-2/IL-18 between ATL patients and elderly non-ATL patients (Figure 5). The proportions of Vδ2$^+$ T cells in CD3$^+$ T cells in the peripheral blood of ATL patients were clearly low, possibly due to both aging and HTLV-1 infection status, while the proportion of Vδ1$^+$ cells in CD3$^+$ T cells remained unchanged, regardless of age and HTLV-1 infection status. However, with the exception of a few cases with extremely low levels of Vδ2$^+$ T cells in CD3$^+$ lymphocyte fractions, the expansion rates of Vδ2$^+$ T cells from elderly, non-ATL patients were comparable to that of HDs and ATL patients (see also Figure 3B). No significant differences in the expression levels of CD16, NKG2D, DNAM-1, FasL, TRAIL, and PD-1 were observed between ATL patients and elderly non-ATL-patients.

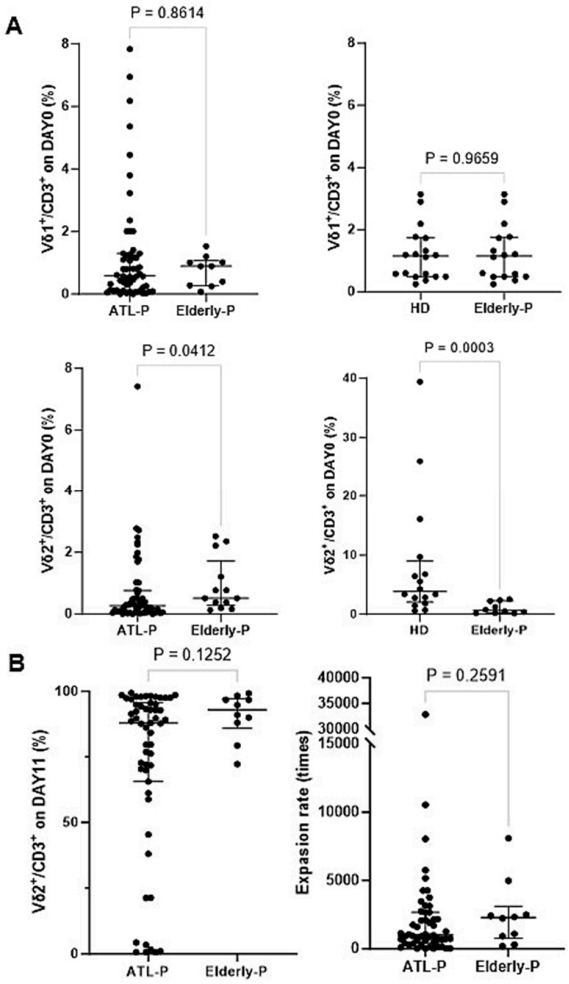

Figure 5. Comparison of PTA/IL-2/IL-18-mediated expansion of γδ T cells among ATL patients, elderly non-ATL patients, and HDs. (**A**) Proportions of Vδ1$^+$ T cells and Vδ2$^+$ T cells in CD3$^+$ T cells before expansion; these initial proportions were compared among the three groups. (**B**) Proportion of Vδ2$^+$ T cells in CD3$^+$ T cells after expansion with PTA/IL-2/IL-18, and the expansion rates of the Vδ2$^+$ T cells were compared between ATL patients and elderly non-ATL patients.

We next stimulated $CD3^-$ PBMC fractions derived from elderly non-ATL patients with IL-2/IL-18 for 10 days (see Supplementary Note added to Result Section 3.5), and compared cell surface markers before and after expansion among ATL patients, elderly non-ATL patients, and HDs (Figure 6). The proportions of NK cells in peripheral blood remained unchanged regardless of age and/or HTLV-1 infection status. After expansion with IL-2/IL-18, highly purified NK cells were obtained from $CD3^-$ PBMC fractions of ATL patients, which was not influenced by age and/or HTLV-1 infection status. However, the expansion rate of NK cells in ATL patients tended to be low, compared to that in HDs, which might be due to aging and HTLV-1 infection status. No significant differences in the expression of CD16, NKG2D, DNAM-1, and CD86 were found between ATL patients and elderly patients.

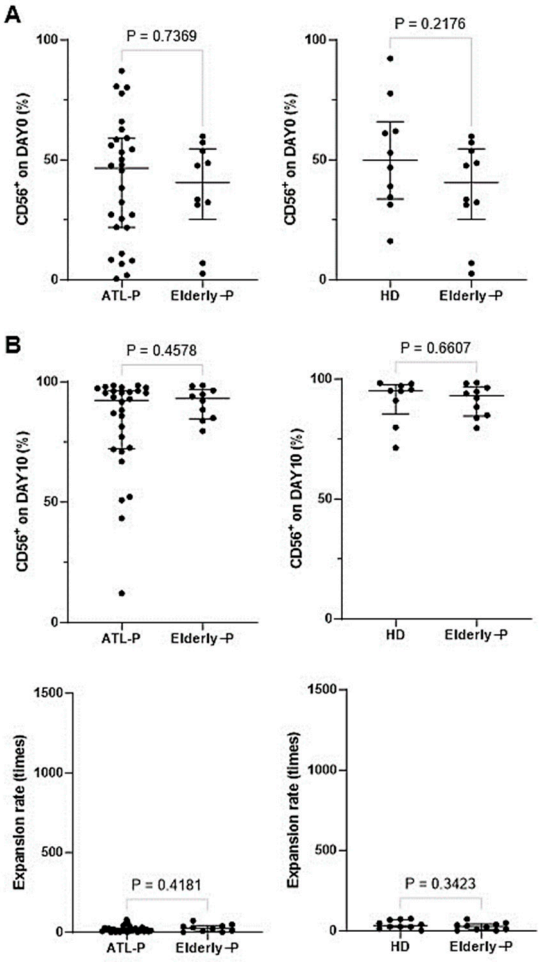

Figure 6. Comparison of NK cells among ATL patients, elderly non-ATL patients, and HDs. (**A**) Initial proportion of NK cells before expansion. The initial proportions of $CD56^+$ cells in PBMCs were compared among the three groups. (**B**) Proportion of NK cells after expansion with IL-2/IL-18. After the expansion, the proportions of $CD56^+$ cells were compared among the three groups.

3.6. Cytotoxic Activity Exhibited by γδ T Cells and NK Cells Derived from ATL Patients against ATL Cell Lines In Vitro

We next examined the cytotoxic activity of PTA/IL-2/IL-18-stimulated/expanded PBMCs containing γδ T cells and NK cells against KK1 and HuT102 HTLV-1-infected cells. After expansion of PBMCs derived from ATL patients with PTA/IL-2/IL-18, cell surface expressions of CD3, CD56, CD16, and Vδ2 were examined. As shown in Supplementary Figure S6, the proportions of γδ T cells, NK cells, and CD16-positive cells varied to different degrees among ATL patients.

When KK1 or HuT102 cells were challenged by PTA/IL-2/IL-18-stimulated/expanded PBMCs containing various proportions of γδ T cells and NK cells, the specific lysis (%) reached 30% to 80% in 60 min at an E/T ratio of 1:200 (Figure 7). By adding 0.5 or 10 μg/mL of anti-CCR4 mAb, the specific lysis increased up to 40–80%, even at an E/T ratio of 1:100. It was worthy of note that the effect of anti-CCR4 mAb on the cellular cytotoxicity was associated with the proportion of γδ T cells, which was consistent with the observation in Figs. 1 and 2. Although the cytotoxicity of NK cells is higher than that of γδ T cells, the addition of anti-CCR4 mAb bolsters the cytotoxic activity of γδ T cells more efficiently, resulting in similar levels of cytotoxicity exhibited by the PTA/IL-2/IL-18-expanded γδ T cell and NK cell mixtures against HTLV-1-infected cells, even if the proportions of γδ T cells and NK cells vary to different degrees.

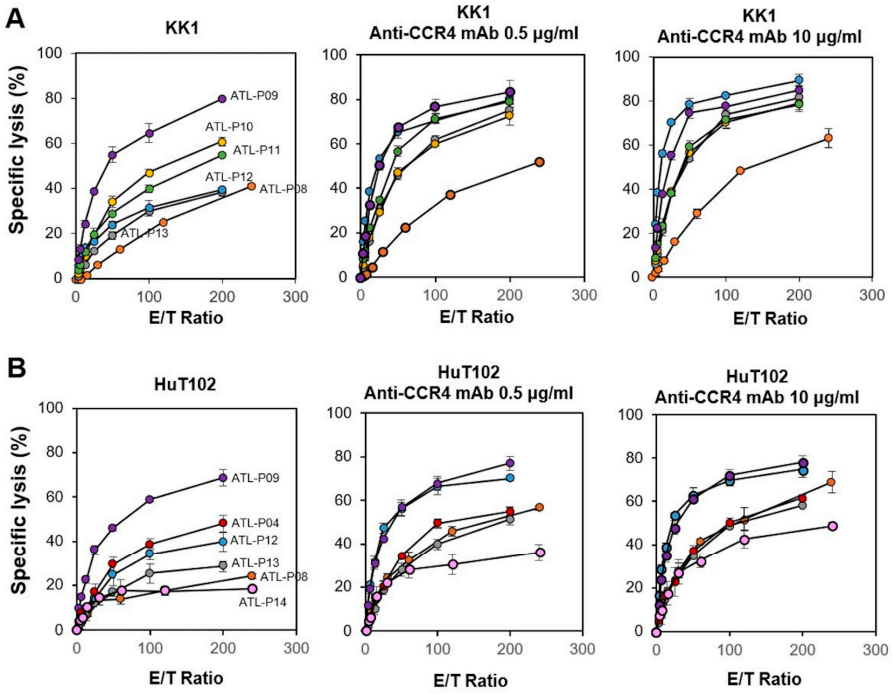

Figure 7. Cytotoxic activity exhibited by γδ T cells and NK cells derived from ATL patients against HTLV-1-infected cells. Effect of anti-CCR4 mAb on the cytotoxic activity of γδ T cells against KK1 (**A**) and HuT102 (**B**). After HTLV-1-infected cell lines were pretreated with 0, 0.5, or 10 μg/mL of anti-CCR4 mAb for 15 min, the sensitized cells were challenged with PTA/IL-2/IL-18-stimulated/expanded γδ T cells and NK cells derived from patients ATL-P04 and ATL-P08-14 at E/T ratios of 3.75:1, 7.5:1, 15:1, 30:1, 60:1, 120:1, and 250:1 or 3.125:1, 6.25:1, 12.5:1, 25:1, 50:1, 100:1, and 200:1 for 60 min, and the specific lysis was determined through a time-resolved fluorescence-based assay based on an europium–terpyridine derivative chelate.

We next examined the cytotoxic activity of IL-2/IL-18-expanded NK cells derived from ATL patients against HTLV-1-infected cells (Figure 8). Flow cytometric diagrams of representative expansion patterns are depicted in Supplementary Figure S7. When KK1 and HuT102 were challenged by IL-2/IL-18-expanded NK cells derived from ATL patients, the specific lysis reached to 20% to 80% in 60 min at an E/T ratio of 1:100. By addition of 0.5 or 10 μg/mL of anti-CCR4 mAb, the specific lysis was increased to 60–90% at an E/T ratio of 1:100 as shown in Figure 8. On the basis of these results, NK cells derived from ATL patients exhibited a highly potent and stable cytotoxicity against HTLV-1-infected cells, as in the case of HDs. Taken together, it is most likely that the PTA/IL-2/IL-18-expanded γδ T cells and NK cells are ideal immune effector cells for adoptive cell therapy against ATL.

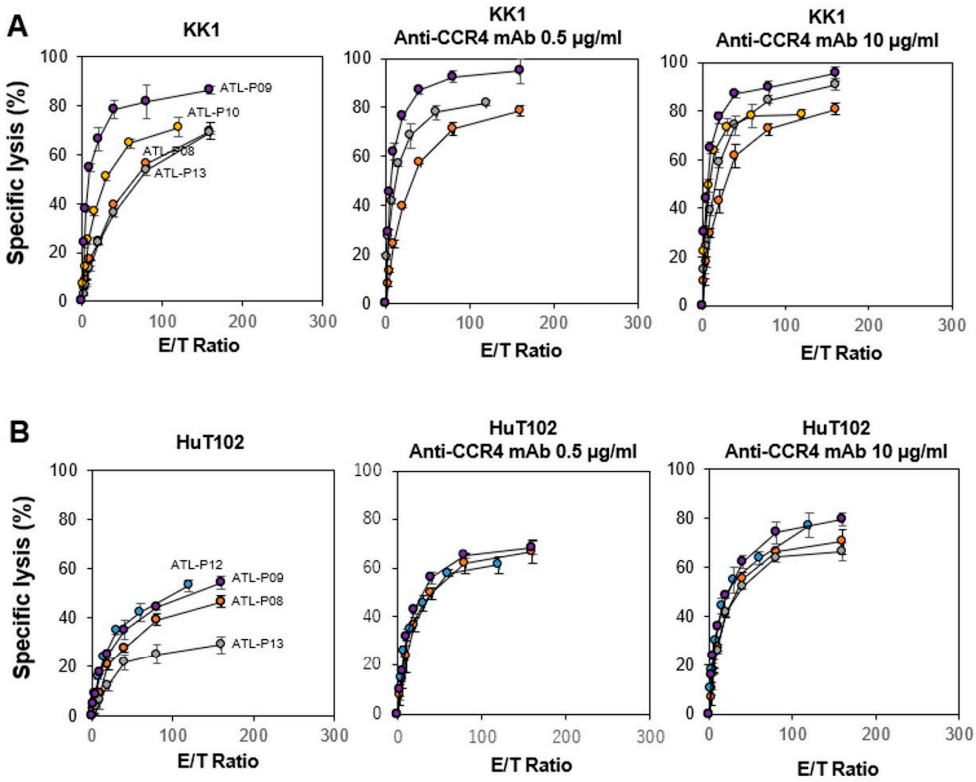

Figure 8. Effect of anti-CCR4 mAb on the cytotoxic activity of NK cells derived from ATL patients against KK1 (**A**) and HuT102 (**B**). After HTLV-1-infected cell lines were pretreated with 0, 0.5, or 10 μg/mL of anti-CCR4 mAb for 15 min, the sensitized cells were challenged with IL-2/IL-18-stimulated/expanded NK cells derived from patients ATL-P08-10 andATL-P12-13 at E/T ratios of 1.875:1, 3.75:1, 7.5:1, 15:1, 30:1, 60:1, and 120:1 or 2.5:1, 5:1, 10:1, 20:1, 40:1, 80:1, and 160:1 for 60 min, and the specific lysis was determined using a time-resolved fluorescence-based assay based on an europium–terpyridine derivative chelate.

4. Discussion

Although infusion therapies for ATL using innate immune cells, such as NK cells [26] and CAR iNKT cells [73], have been developed extensively over the past few years, it is still a long way off from clinical use in terms of their efficacy and cost. In this study, we explored the possibility of the development of γδ T cells/NK cells-based adoptive transfer therapy for ATL.

γδ T cells belong to both innate immunity and adaptive immunity and are involved in the first line of defense against cancer including solid tumors [34–45] and lymphoid malignancies [74]. Previous reports [50] and the present study demonstrated that γδ T cells could be readily amplified in HDs and the expanded γδ T cells exhibited potent cytotoxicity against HTLV-1-infected cells. ATL patients are, however, generally elderly and infected with HTLV-1 viruses, and the immune system in ATL patients is mostly suppressed [24–26]. Thus, our primary question was how aging and the state of immunosuppression affect the expansion and immunological properties of γδ T cells.

It was noteworthy that the proportion of peripheral blood γδ T cells from ATL patients was extremely low, with the median proportion of γδ T cells being 0.29% (range: 0.0–7.41%). In fact, the initial frequency of γδ T cells in $CD3^+$ lymphocyte fractions was less than 0.1% in 29.6% of ATL patients, whereas such a low frequency of γδ T cells was observed only in 10% of elderly non-ATL patients and 0% of HDs. On the basis of these findings, the low proportion of peripheral blood γδ T cells seemed to be attributable to aging and the state of immunosuppression. In fact, when the state of ATL disease was worse in terms of clinical indicators and aggressive diagnoses in Shimoyama classification, the proportion of γδ T

cells in the peripheral blood tended to be lower. It was, however, worthy of note that the expansion rate of γδ T cells in ATL patients was comparable to that of HDs. Even if the expansion rate is high enough, the initial proportion directly affects the number of γδ T cells after expansion, leading to a difficulty in the preparation of a large number of γδ T cells ex vivo. It is, therefore, prerequisite to develop a strategy to increase the number of γδ T cells more efficiently.

It was previously demonstrated that IL-18 could efficiently augment the expansion of γδ T cells and NK cells with potent cytotoxicity [51–53]. When PBMCs were incubated with IL-18 in addition to PTA/IL-2, the expansion rate of the γδ T cells was significantly greater than that with PTA/IL-2. In addition, NK cells were also expanded in the culture due to the presence of IL-2/IL-18. Although NK cells increased in number with stimulation using IL-2/IL-18, the expansion rate was generally low compared to that of the γδ T cells, even in HDs. The present study demonstrated that NK cell proliferation, itself, tended to reduce with aging, whereas the expressions of NKG2D, DNAM-1, CD16, HLA-DQ, and CD86 remained unchanged.

Although γδ T cells failed to proliferate well even in the presence of PTA/IL-2/IL-18, in some cases, an increase in the number of NK cells was observed, instead, in the culture, suggesting that the NK cells were complementarily expanded when the initial proportion of γδ T cells was extremely low. Since NK cells also exhibit anti-ATL activity, we should consciously examine the expansion of NK cells in culture that is intended to expand γδ T cells for use in adoptive cell therapy.

We next examined the cytotoxicity of the expanded innate immune effector cells against HTLV-1-infected cells. When HTLV-1-infected cells were challenged by γδ T cells and NK cells, the direct cytotoxicity exhibited by NK cells was much higher than that by γδ T cells, suggesting that the NK cells were superior to the γδ T cells as effector cells in terms of cytotoxicity. It is, however, difficult to prepare a large number of NK cells for use in infusion therapy, compared to γδ T cells, indicating that γδ T cells are superior to NK cells when it comes to the preparation of effector cells. There are advantages and disadvantages to both cell types.

In studies on the effect of IL-18 on the anti-CD20 mAb-mediated regression of non-Hodgkin lymphoma, it was demonstrated that IL-18 synergized with the mAb in the lymphoma regression [75]. Since both NK cells and γδ T cells express CD16, it is intriguing to examine whether ADCC plays a certain role in the regression. As for ATL, HTLV-1-infected cells express a high level of CCR4, implicating that the inclusion of anti-CCR4 mAb might enhance the cytotoxic activity of NK cells and γδ T cells. When the cytotoxic activity of the mixture of γδ T cells and NK cells derived from ATL patients was measured, the immune effector cell mixtures exhibited high levels of cellular cytotoxicity against HTLV-1-infected cells to different degrees. When anti-CCR4 mAb was added to the system, the cytotoxicity was enhanced to different degrees, depending on the proportion of γδ T cells. When the proportion of γδ T cells was relatively high, the add-on effect of the mAb was more prominent, suggesting that ADCC mediated by γδ T cells was more efficient than that by NK cells, since the direct killing of HTLV-1-infected cells by NK cells was intrinsically high even in the absence of the ADCC pathway.

In this study, it was clearly demonstrated that HTLV-1-infected cells were susceptible to the cytotoxic activity of γδ T cells in vitro, which was further enhanced by the addition of anti-CCR4 mAb. In addition, NK cells exhibited potent cytotoxicity against HTLV-1-infected cells even in the absence of mAbs. In order to move on to clinical trials, the present in vitro findings should be confirmed in animal models using an immunocompromised mouse model. In this study, three ATL patients failed to respond to PTA/IL-2/IL-18 at all. In these patients, the proportion and the number of HTLV-1-infected cells were too high and the cell culture for the expansion of NK cells and γδ T cells could not be appropriately set up. It should be thus considered that the removal of HTLV-1-infected cells should be included in the protocol for the expansion of NK cells and γδ T cells.

Since the present study was only a preliminary investigation to evaluate the feasibility of adoptive transfer therapy harnessing γδ T cells and NK cells, an autologous system was considered, with the safety of the treatment being the most important issue. The adoptive transfer of allogeneic γδ T cells is more practically promising, because it is much easier to expand γδ T cells and NK cells derived from HDs. In fact, γδ T cells and NK cells derived from HDs could be adoptively transferred into elderly and immunocompromised ATL patients, because the γδ T cell- and NK cell-mediated cytotoxicity is not restricted by the MHC molecules. It is, however, essential to conduct clinical trials carefully and extensively for the development of such allogeneic innate immune effector cell-based infusion therapy for ATL. Taken together, autologous γδ T cells and NK cells could be utilized for the treatment of ATL. If the safety and efficacy of allogeneic γδ T cells and NK cells is proven in clinical trials, γδ T cells and NK cells derived from HDs could be used together with anti-CCR4 mAb for the treatment of ATL as an over-the-counter treatment in the near future.

5. Conclusions

In this study, we have shown the potential of a new therapeutic strategy for ATL. In the future, we would like to conduct in vivo studies in a clinical setting and create a system that enables allogeneic γδ T cell transplantation.

Supplementary Materials: The following supporting information can be downloaded at https://www.mdpi.com/article/10.3390/cells13020128/s1: Figure S1: Expansion of γδ T cells from HDs with PTA/IL-2; Figure S2: Expansion of NK cells from HDs with IL-2/IL-18; Figure S3: Expansion with PTA/IL-2/Il-18 of γδ T cells and NK cells derived from ATL patients; Figure S4: Effect of PTA/IL-2/Il-18 on the expansion of γδ T cells derived from ATL patients; Figure S5: Expansion with IL-2/IL-18 of NK cells from ATL patients; Figure S6: Expansion with PTA/IL-2/IL-18 of γδ T cells and NK cells derived from ATL patients (ATL-P04, 08-14); Figure S7: Expansion with IL-2/IL-18 of NK cells derived from ATL patients (ATL-P08-10, 12-13); Table S1: Summary of flow cytometric analysis, PTA/IL-2-induced expansion of γδ T cells and IL-2/IL-18-induced expansion of NK cells in HDs; Table S2: Summary of the clinical characteristics of 55 ATL patients; Table S3: The Shimoyama classification at the first diagnosis and the outcome at the time of blood sampling; Table S4; Summary of flow cytometric analysis, PTA/IL-2-induced expansion of γδ T cells, PTA/IL-2/IL-18-induced expansion of γδ T cells and IL-2/IL-18-induced expansion of NK cells in ATL patients; Table S5; Summary of flow cytometric analysis, PTA/IL-2/IL-18-induced expansion of γδ T cells and IL-2/IL-18-induced expansion of NK cells in elderly non-ATL patients.

Author Contributions: M.N., Y.T. and H.M.: Conceptualization, data curation, funding acquisition, investigation, project administration, writing, and editing; H.O., T.K., Y.I., K.N. and Y.M.: resources and editing. All authors have read and agreed to the published version of the manuscript.

Funding: This work was supported by JST START University Ecosystem Promotion Type (Supporting the Creation of Startup Ecosystems in Startup Cities), Japan, grant no. JPMJST2281 to Y.T.; by Grants-in-Aid for Scientific Research from MEXT, grant no. 16K08844 and 23K06677 to Y.T.; by Grants-in-Aid for Scientific Research from the Japan Agency for Medical Research and Development, grant no. A48 and A90 to Y.T.; and by Research Funding granted by Nagasaki University President Shigeru Kohno to Y.T. The contents of this manuscript are solely the responsibility of the authors and do not necessarily represent the official views of the granting agencies.

Institutional Review Board Statement: This study was approved by the Nagasaki University Hospital Clinical Research Ethics Committee (13022512 and UMIN000042835).

Informed Consent Statement: Informed consent was obtained from all subjects involved in the study. Written informed consent was obtained from the patients to publish this paper.

Data Availability Statement: The raw data supporting the conclusions of this article will be made available by the authors, without undue reservation.

Acknowledgments: We would like to thank Chigusa Tanaka and Miho Soma for technical assistance.

Conflicts of Interest: Y.T. is a co-inventor of JP2014-257451 (on the method for expanding γδ T cells using PTA) and JP2014-73475 (on the method for a nonradioactive cellular cytotoxicity assay). Y.M. has received honoraria for speaker bureaus from SymBio Pharmaceuticals Limited, Novartis Pharma K.K.; AbbVie Inc.; Nippon Shinyaku Co., Ltd.; Astellas Pharma Inc.; and Sumitomo Pharma Co., Ltd. Y.M. received a research grant from Chugai Pharmaceutical Co., Ltd. Y.I. received honoraria for speaker bureaus from SymBio Pharmaceuticals Limited; Bristol-Myers Squibb K.K.; Daiichi Sankyo Company, Limited; AstraZeneca K.K.; Sanofi K.K.; Meiji Seika Pharma Co., Ltd.; and Chugai Pharmaceutical Co., Ltd. The other authors declare that the research was conducted in the absence of any commercial or financial relationships that could be construed as a potential conflict of interest.

References

1. Uchiyama, T.; Yodoi, J.; Sagawa, K.; Takatsuki, K.; Uchino, H. Adult T-cell leukemia: Clinical and hematologic features of 16 cases. *Blood* **1977**, *50*, 481–492. [CrossRef] [PubMed]
2. Takatsuki, K. Discovery of adult T-cell leukemia. *Retrovirology* **2005**, *2*, 16. [CrossRef]
3. Gessain, A.; Cassar, O. Epidemiological Aspects and World Distribution of HTLV-1 Infection. *Front. Microbiol.* **2012**, *3*, 388. [CrossRef] [PubMed]
4. Satake, M.; Yamaguchi, K.; Tadokoro, K. Current prevalence of HTLV-1 in Japan as determined by screening of blood donors. *J Med Virol.* **2012**, *84*, 327–335. [CrossRef] [PubMed]
5. Satake, M.; Iwanaga, M.; Sagara, Y.; Watanabe, T.; Okuma, K.; Hamaguchi, I. Incidence of human T-lymphotropic virus 1 infection in adolescent and adult blood donors in Japan: A nationwide retrospective cohort analysis. *Lancet Infect. Dis.* **2016**, *16*, 1246–1254. [CrossRef]
6. Ito, S.; Iwanaga, M.; Nosaka, K.; Imaizumi, Y.; Ishitsuka, K.; Amano, M.; Utsunomiya, A.; Tokura, Y.; Watanabe, T.; Uchimaru, K.; et al. Epidemiology of adult T-cell leukemia-lymphoma in Japan: An updated analysis, 2012–2013. *Cancer Sci.* **2021**, *112*, 4346–4354. [CrossRef] [PubMed]
7. Iwanaga, M. Epidemiology of HTLV-1 infection and ATL in Japan: An update. *Front. Microbiol.* **2020**, *29*, 1124. [CrossRef]
8. Shimoyama, M. Diagnostic criteria and classification of clinical subtypes of adult T-cell leukaemia-lymphoma. A report from the Lymphoma Study Group (1984-87). *Br. J. Haematol.* **1991**, *79*, 428–437. [CrossRef]
9. Tsukasaki, K.; Hermine, O.; Bazarbachi, A.; Ratner, L.; Ramos, J.C.; Harrington, W., Jr.; O'Mahony, D.; Janik, J.E.; Bittencourt, A.L.; Taylor, G.P.; et al. Definition, prognostic factors, treatment, and response criteria of adult T-cell leukemia-lymphoma: A proposal from an international consensus meeting. *J. Clin. Oncol.* **2009**, *27*, 453–459. [CrossRef]
10. Ishida, T.; Itoh, A.; Tokura, Y.; Tanaka, J.; Uike, N.; Tobinai, K.; Tsukasaki, K. An integrated manual for hematologists and dermatologists to access the guidelines for the management of adult T-cell leukemia-lymphoma (2014). *Rinsho Ketsueki* **2014**, *55*, 2257–2261.
11. Utsunomiya, A.; Miyazaki, Y.; Takatsuka, Y.; Hanada, S.; Uozumi, K.; Yashiki, S.; Tara, M.; Kawano, F.; Saburi, Y.; Kikuchi, H.; et al. Improved outcome of adult T cell leukemia/lymphoma with allogeneic hematopoietic stem cell transplantation. *Bone Marrow Transpl.* **2001**, *27*, 15–20. [CrossRef] [PubMed]
12. Utsunomiya, A.; Choi, I.; Chihara, D.; Seto, M. Recent advances in the treatment of adult T-cell leukemia-lymphomas. *Cancer Sci.* **2015**, *106*, 344–351. [CrossRef] [PubMed]
13. Shichijo, T.; Nosaka, K.; Tatetsu, H.; Higuchi, Y.; Endo, S.; Inoue, Y.; Toyoda, K.; Kikukawa, Y.; Kawakita, T.; Yasunaga, J.; et al. Beneficial impact of first-line mogamulizumab-containing chemotherapy in adult T-cell leukaemia-lymphoma. *Br. J. Hematol.* **2022**, *198*, 983–987. [CrossRef] [PubMed]
14. Nakashima, J.; Imaizumi, Y.; Taniguchi, H.; Ando, K.; Iwanaga, M.; Itonaga, H.; Sato, S.; Sawayama, Y.; Hata, T.; Yoshida, S.; et al. Clinical factors to predict outcome following mogamulizumab in adult T-cell leukemia-lymphoma. *Int. J. Hematol.* **2018**, *108*, 516–523. [CrossRef] [PubMed]
15. Ogura, M.; Imaizumi, Y.; Uike, N.; Asou, N.; Utsunomiya, A.; Uchida, T.; Aoki, T.; Tsukasaki, K.; Taguchi, J.; Choi, I.; et al. Lenalidomide in relapsed adult T-cell leukemia-lymphoma or peripheral T-cell lymphoma (ATLL-001): A phase 1, multicentre, dose-escalation study. *Lancet Hematol.* **2016**, *3*, 107–118. [CrossRef]
16. Imaizumi, Y.; Iwanaga, M.; Nosaka, K.; Ishitsuka, K.; Ishizawa, K.; Ito, S.; Amano, M.; Ishida, T.; Uike, N.; Utsunomiya, A.; et al. Prognosis of patients with adult T-cell leukemia/lymphoma in Japan: A nationwide hospital-based study. *Cancer Sci.* **2020**, *111*, 4567–4580. [CrossRef]
17. Hishizawa, M.; Kanda, J.; Utsunomiya, A.; Taniguchi, S.; Eto, T.; Moriuchi, Y.; Tanosaki, R.; Kawano, F.; Miyazaki, Y.; Masuda, M.; et al. Transplantation of allogeneic hematopoietic stem cells for adult T-cell leukemia: A nationwide retrospective study. *Blood* **2010**, *116*, 1369–1376. [CrossRef]
18. Nosaka, K.; Iwanaga, M.; Imaizumi, Y.; Ishitsuka, K.; Ishizawa, K.; Ishida, Y.; Amano, M.; Ishida, T.; Uike, N.; Utsunomiya, A.; et al. Epidemiological and clinical features of adult T-cell leukemia-lymphoma in Japan, 2010–2011, a nationwide survey. *Cancer Sci.* **2017**, *108*, 2478–2486. [CrossRef]
19. Kinosada, H.; Yasunaga, J.I.; Shimura, K.; Miyazato, P.; Onishi, C.; Iyoda, T.; Inaba, K.; Matsuoka, M. HTLV-1 bZIP Factor Enhances T-Cell Proliferation by Impeding the Suppressive Signaling of Co-inhibitory Receptors. *PLoS Pathog.* **2017**, *13*, 1006120.

20. Watanabe, T. Adult T-cell leukemia: Molecular basis for clonal expansion and transformation of HTLV-1-infected T cells. *Blood* **2017**, *129*, 1071–1081. [CrossRef]
21. Yamagishi, M.; Fujikawa, D.; Watanabe, T.; Uchimaru, K. HTLV-1-Mediated Epigenetic Pathway to Adult T-Cell Leukemia-Lymphoma. *Front. Microbiol.* **2018**, *9*, 1686. [CrossRef] [PubMed]
22. Mahgoub, M.; Yasunaga, J.; Iwami, S.; Nakaoka, S.; Koizumi, Y.; Shimura, K.; Matsuoka, M. Sporadic on/off switching of HTLV-1 Tax expression is crucial to maintain the whole population of virus-induced leukemic cells. *Proc. Natl. Acad. Sci. USA* **2018**, *115*, E1269–E1278. [CrossRef] [PubMed]
23. Kataoka, K.; Koya, J. Clinical application of genomic aberrations in adult T-cell leukemia/lymphoma. *J. Clin. Exp. Hematol.* **2020**, *60*, 66–72. [CrossRef] [PubMed]
24. Azakami, K.; Sato, T.; Araya, N.; Utsunomiya, A.; Kubota, R.; Suzuki, K.; Hasegawa, D.; Izumi, T.; Fujita, H.; Aratani, S.; et al. Severe loss of invariant NKT cells exhibiting anti–HTLV-1 activity in patients with HTLV-1-associated disorders. *Blood* **2009**, *114*, 3208–3215. [CrossRef]
25. Ogura, M.; Ishida, T.; Tsukasaki, K.; Takahashi, T.; Utsunomiya, A. Effects of first-line chemotherapy on natural killer cells in adult T-cell leukemia–lymphoma and peripheral T-cell lymphoma. *Cancer Chemother. Pharmacol.* **2016**, *78*, 199–207. [CrossRef]
26. Nagai, K.; Nagai, S. Effectiveness of Amplified Natural Killer (ANK) Therapy for Adult T-cell Leukemia/Lymphoma (ATL) and Future Prospects of ANK Therapy. *Cancer Med. J.* **2022**, *5*, 27–33. [PubMed]
27. Wu, Y.; Tian, Z.; Wei, H. Developmental and Functional Control of Natural Killer Cells by Cytokines. *Front. Immunol.* **2017**, *8*, 930. [CrossRef]
28. Choi, Y.H.; Lim, E.J.; Kim, S.W.; Moon, Y.W.; Parket, K.S.; An, H.J. IL-27 enhances IL-15/IL-18-mediated activation of human natural killer cells. *J. Immunother. Cancer* **2019**, *7*, 168. [CrossRef]
29. Wrona, E.; Borowiec, M.; Potemski, P. CAR-NK Cells in the Treatment of Solid Tumors. *Int. J. Mol. Sci.* **2021**, *22*, 5899. [CrossRef]
30. Conlon, K.C.; Potter, E.L.; Pittaluga, S.; Lee, C.R.; Miljkovic, M.D.; Fleisher, T.A.; Dubois, S.; Bryant, B.R.; Petrus, M.; Perera, L.P.; et al. IL15 by Continuous Intravenous Infusion to Adult Patients with Solid Tumors in a Phase I Trial Induced Dramatic NK-Cell Subset Expansion. *Clin. Cancer Res.* **2019**, *25*, 4945–4954. [CrossRef]
31. June, C.H.; O'Connor, R.S.; Kawalekar, O.U.; Ghassemi, S.; Milone, M.C. CAR T cell immunotherapy for human cancer. *Science* **2018**, *359*, 1361–1365. [CrossRef]
32. Schuster, S.J.; Svoboda, J.; Chong, E.A.; Nasta, S.D.; Mato, A.R.; Anak, Ö.; Brogdon, J.L.; Pruteanu-Malinici, I.; Bhoj, V.; Landsburg, D.; et al. Chimeric Antigen Receptor T Cells in Refractory B-Cell Lymphomas. *N. Engl. J. Med.* **2017**, *377*, 2545–2554. [CrossRef] [PubMed]
33. Sterner, R.C.; Sterner, R.M. CAR-T cell therapy: Current limitaions and potential strategies. *Blood Cancer J.* **2021**, *11*, 69. [CrossRef] [PubMed]
34. Zocchi, M.R.; Poggi, A. Role of gammadelta T lymphocytes in tumor defense. *Front. Biosci.* **2004**, *9*, 2588–2604. [CrossRef] [PubMed]
35. Kabelitz, D.; Wesch, D.; Pitters, E.; Zöller, M. Characterization of Tumor Reactivity of Human Vγ9Vδ2 γδ T Cells In Vitro and in SCID Mice In Vivo. *J. Immunol.* **2004**, *173*, 6767–6776. [CrossRef]
36. Kabelitz, D.; Wesch, D.; He, W. Perspectives of γδ T Cells in Tumor Immunology. *Cancer Res.* **2007**, *67*, 5–8. [CrossRef]
37. Hayday, A.C. γδ CELLS: A Right Time and a Right Place for a Conserved Third Way of Protection. *Annu. Rev. Immunol.* **2000**, *18*, 975–1026. [CrossRef]
38. Fournie, J.J.; Sicard, H.; Poupot, M.; Bezombes, C.; Blanc, A.; Romagné, F.; Ysebaert, L.; Laurent, G. What lessons can be learned from γδ T cell-based cancer immunotherapy trials? *Cell. Mol. Immunol.* **2013**, *10*, 35–41. [CrossRef]
39. Bonneville, M.; O'Brien, R.L.; Born, W.K. γδ T cell effector functions: A blend of innate programming and acquired plasticity. *Nat. Rev. Immunol.* **2010**, *10*, 467–478. [CrossRef]
40. Bonneville, M.; Scotet, E. Human Vgamma9Vdelta2 T cells: Promising new leads for immunotherapy of infections and tumors. *Curr. Opin. Immunol.* **2006**, *18*, 539–546. [CrossRef]
41. Scotet, E.; Martinez, L.O.; Grant, E.; Barbaras, R.; Jenö, P. Tumor Recognition following Vγ9Vδ2 T Cell Receptor Interactions with a Surface F1-ATPase-Related Structure and Apolipoprotein A-I. *Immunity* **2005**, *22*, 71–80. [CrossRef] [PubMed]
42. Silva-Santos, B.; Serre, K.; Norell, H. γδ T cells in cancer. *Nat. Rev. Immunol.* **2015**, *15*, 683–691. [CrossRef]
43. Mensurado, S.; Blanco-Domínguez, R.; Silva-Santos, B. The emerging roles of γδ T cells in cancer immunotherapy. *Nat. Rev. Clin. Oncol.* **2023**, *20*, 178–191. [CrossRef] [PubMed]
44. Cerapio, J.P.; Perrier, M.; Balança, C.C.; Gravellea, P.; Pont, F. Phased differentiation of γδ T and T CD8 tumor-infiltrating lymphocytes revealed by single-cell transcriptomics of human cancers. *Oncoimmunology* **2021**, *10*, e1939518. [CrossRef] [PubMed]
45. Lawrence, S.; Lamb, J.R. γδ T cells as immune effectors against high-grade gliomas. *Immunol. Res.* **2009**, *45*, 85–95.
46. Porcelli, S.; Brenner, M.B.; Band, H. Biology of human γδ T cell receptor. *Immunol. Rev.* **1991**, *120*, 137–183. [CrossRef]
47. Constant, P.; Davodeau, F.; Peyrat, M.A.; Poquet, Y.; Puzo, G.; Bonneville, M.; Fournié, J.J. Stimulation of human gamma delta T cells by nonpeptidic mycobacterial ligands. *Science* **1994**, *264*, 267–270. [CrossRef]
48. Tanaka, Y.; Morita, C.T.; Tanaka, Y.; Nieves, E.; Brenner, M.B.; Bloom, B.R. Natural and synthetic non-peptide antigens recognized by human gamma delta T cells. *Nature* **1995**, *375*, 155–158. [CrossRef]

49. Puan, K.J.; Jin, C.; Wang, H.; Sarikonda, G.; Raker, A.M.; Lee, H.K.; Samuelson, M.I.; Märker-Hermann, E.; Pasa-Tolic, L.; Nieves, E.; et al. Preferential recognition of a microbial metabolite by human Vg2Vd2 T cells. *Int. Immunol.* **2007**, *19*, 657–673. [CrossRef]
50. Tanaka, Y.; Murata-Hirai, K.; Iwasaki, M.; Matsumoto, K.; Hayashi, K.; Kumagai, A.; Nada, M.H.; Wang, H.; Kobayashi, H.; Kamitakahara, H.; et al. Expansion of human γδ T cells for adoptive immunotherapy using a bisphosphonate prodrug. *Cancer Sci.* **2018**, *109*, 587–599. [CrossRef]
51. Li, Y.; Wu, H.-W.; Sheard, M.A.; Sposto, R.; Somanchi, S.S.; Cooper, L.J.N.; Lee, D.A.; Seeger, R.C. Growth and activation of natural killer cells ex vivo from children with neuroblastoma for adoptive therapy. *Clin. Cancer Res.* **2013**, *19*, 2132–2143. [CrossRef] [PubMed]
52. Li, W.; Yamamoto, H.; Kubo, S.; Okamura, H. Modulation of innate immunity by IL-18. *J. Rep. Immunol.* **2009**, *83*, 101–105. [CrossRef] [PubMed]
53. Yasuda, K.; Nakanishi, K.; Tsutsui, H. Interleukin-18 in Health and Disease. *Int. J. Mol. Sci.* **2019**, *20*, 649. [CrossRef] [PubMed]
54. Ishida, T.; Utsunomiya, A.; Iida, S.; Inagaki, H.; Takatsuka, Y.; Kusumoto, S.; Takeuchi, G.; Shimizu, S.; Ito, M.; Komatsu, H.; et al. Clinical significance of CCR4 expression in adult T-cell leukemia/lymphoma: Its close association with skin involvement and unfavorable outcome. *Clin. Cancer Res.* **2003**, *9*, 3625–3634.
55. Ishii, T.; Ishida, T.; Utsunomiya, A.; Inagaki, A.; Yano, H.; Komatsu, H.; Iida, S.; Imada, K.; Uchiyama, T.; Akinaga, S.; et al. Defucosylated humanized anti-CCR4 monoclonal antibody KW-0761 as a novel immuno-therapeutic agent for adult T-cell leukemia/lymphoma. *Clin. Cancer Res.* **2010**, *16*, 1520–1531. [CrossRef] [PubMed]
56. Tanaka, H.; Fujiwara, H.; Ochi, F.; Tanimoto, K.; Casey, N.; Okamoto, S.; Mineno, J.; Kuzushima, K.; Shiku, H.; Sugiyama, T.; et al. Development of Engineered T Cells Expressing a Chimeric CD16-CD3ζ Receptor to Improve the Clinical Efficacy of Mogamulizumab Therapy Against Adult T-Cell Leukemia. *Clin. Cancer Res.* **2016**, *22*, 4405–4416. [CrossRef]
57. Couzi, L.; Pitard, V.; Sicard, X.; Garrigue, I.; Hawchar, O.; Merville, P.; Moreau, J.F.; Déchanet-Merville, J. Antibody-dependent anti-cytomegalovirus activity of human γδ T cells expressing CD16 (Fcγ RIIIa). *Blood* **2012**, *119*, 1418–1427. [CrossRef] [PubMed]
58. Capietto, A.H.; Martinet, L.; Fournie, J.J. Stimulated γδ T cells increase the in vivo efficacy of trastuzumab in HER-2+ breast cancer. *J. Immunol.* **2011**, *187*, 1031–1038. [CrossRef]
59. Besser, M.J.; Shoham, T.; Fournie, J.J.; Harari-Steinberg, O.; Zabari, N.; Ortenberg, R.; Yakirevitch, A.; Nagler, A.; Loewenthal, R.; Schachter, J.; et al. Development of allogeneic NK cell adoptive transfer therapy in metastatic melanoma patients: In vitro preclinical optimization studies. *PLoS ONE* **2013**, *8*, e57922.
60. Yssel, H.; De Vries, J.E.; Koken, M.; Blitterswijk, W.V.; Spits, H. Serum-free medium for generation and propagation of functional human cytotoxic and helper T cell clones. *J. Immunol. Methods* **1984**, *72*, 219–227. [CrossRef]
61. Han, S.; Georgiev, P.; Ringel, A.E.; Sharpe, A.H.; Haigis, M.C. Age-associated remodeling of T cell immunity and metabolism. *Cell Metab.* **2023**, *35*, 36–55. [CrossRef] [PubMed]
62. Pietschmann, K.; Beetz, S.; Welte, S.; Gruen, J.; Oberg, H.H.; Wesch, D.; Kabelitz, D. Toll-like receptor expression and function in subsets of human gammadelta T lymphocytes. *Scand J. Immunol.* **2009**, *70*, 245–255. [CrossRef]
63. Rincon-Orozco, B.; Kunzmann, V.; Wrobel, P.; Kabelitz, D.; Steinle, A.; Herrmann, T. Activation of V gamma 9 V delta 2 T cells by NKG2D. *J. Immunol.* **2005**, *175*, 2144–2151. [CrossRef] [PubMed]
64. Gertner-Dardenne, J.; Bonnafous, C.; Bezombes, C.; Capietto, A.H.; Scaglione, V.; Ingoure, S.; Cendron, D.; Gross, E.; Lepage, J.F.; Quillet-Mary, A.; et al. Bromohydrin pyrophosphate enhances antibody-dependent cell-mediated cytotoxicity induced by therapeutic antibodies. *Blood* **2009**, *113*, 4875–4884. [CrossRef] [PubMed]
65. Toutirais, O.; Cabillic, F.; Le Friec, G.; Salot, S.; Loyer, P.; Gallo, M.L.; Desille, M.; LaPintie're, C.T.; Daniel, P.; Bouet, F.; et al. DNAX accessory molecule-1 (CD226) promotes human hepatocellular carcinoma cell lysis by Vgamma9Vdelta2 T cells. *Eur. J. Immunol.* **2009**, *39*, 1361–1368. [CrossRef] [PubMed]
66. Stojanovic, A.; Correia, M.P.; Cerwenka, A. The NKG2D/NKG2DL Axis in the Crosstalk Between Lymphoid and Myeloid Cells in Health and Disease. *Front. Immunol.* **2018**, *9*, 827. [CrossRef] [PubMed]
67. Wrobel, P.; Shojaei, H.; Schittek, B.; Gieseler, F.; Wollenberg, B.; Kalthoff, H.; Kabelitz, D.; Wesch, D. Lysis of a broad range of epithelial tumour cells by human gamma delta T cells: Involvement of NKG2D ligands and T-cell receptor- versus NKG2D-dependent recognition. *Scand. J. Immunol.* **2007**, *66*, 320–328. [CrossRef] [PubMed]
68. Iwasaki, M.; Tanaka, Y.; Kobayashi, H.; Murata-Hirai, K.; Miyabe, H.; Sugie, T.; Toi, M.; Minato, N. Expression and function of PD-1 in human γδ T cells that recognize phosphoantigens. *Eur. J. Immunol.* **2011**, *41*, 345–355. [CrossRef]
69. Maeda, M.; Tanabe-Shibuya, J.; Miyazato, P.; Masutani, H.; Yasunaga, J.; Usami, K.; Shimizu, A.; Matsuoka, M. IL-2/IL-2 Receptor Pathway Plays a Crucial Role in the Growth and Malignant Transformation of HTLV-1-Infected T Cells to Develop Adult T-Cell Leukemia. *Front. Microbiol.* **2020**, *11*, 356. [CrossRef]
70. Niehrs, A.; Altfeld, M. Regulation of NK-Cell Function by HLA Class II. *Front. Cell. Infect. Microbiol.* **2020**, *10*, 55. [CrossRef]
71. Zhang, Q.; Ma, R.; Chen, H.; Guo, W.; Li, Z.; Xu, K.; Chen, W. CD86 Is Associated with Immune Infiltration and Immunotherapy Signatures in AML and Promotes Its Progression. *J. Oncol.* **2023**, *2023*, 9988405. [CrossRef] [PubMed]
72. Sakai, Y.; Mizuta, S.; Kumagai, A.; Tagod, M.S.O.; Senju, H.; Nakamura, T.; Morita, C.T.; Tanaka, Y. Live cell labeling with terpyridine derivative proligands to measure cytotoxicity mediated by immune cells. *ChemMedChem* **2017**, *12*, 2006–2013. [CrossRef] [PubMed]
73. Rowan, A.G.; Ponnusamy, K.; Ren, H.; Taylor, G.P.; Cook, L.B.M.; Karadimitris, A. CAR-iNKT cells targeting clonal TCRVβ chains as a precise strategy to treat T cell lymphoma. *Front. Immunol.* **2023**, *14*, 118681. [CrossRef] [PubMed]

74. Kunzmann, V.; Wilhelm, M. Anti-lymphoma effect of gammadelta T cells. *Leuk Lymphoma* **2005**, *46*, 671–680. [CrossRef]
75. Robertson, M.J.; Kline, J.; Struemper, H.; Koch, K.M.; Bauman, J.W.; Gardner, O.S.; Murray, S.C.; Germaschewski, F.; Weisenbach, J.; Jonak, Z.; et al. A dose-escalation study of recombinant human interleukin-18 in combination with rituximab in patients with non-Hodgkin lymphoma. *J. Immunother.* **2013**, *36*, 331–341. [CrossRef]

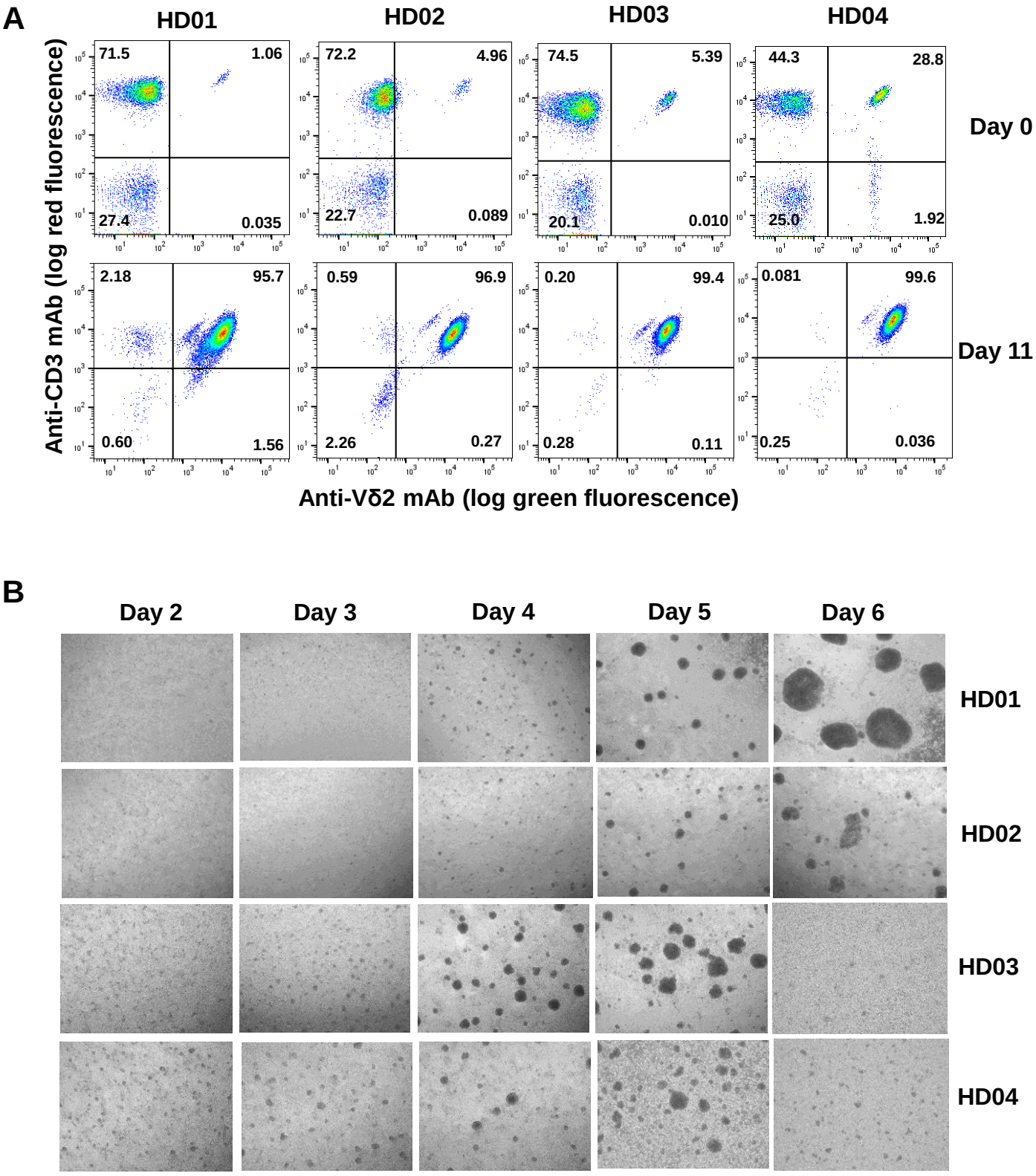

Supplementary Fig. 1. Expansion of γδ T cells from HDs with PTA/IL-2. (A) Flow cytometric analyses of PTA/IL-2-mediated expansion of γδ T cells derived from HDs. Before and after expansion for 11 days with PTA/IL-2, the cells were stained with phycoerythrin (PE)-labeled anti-CD3 mAb and fluorescein isothiocyanate (FITC)-labeled anti-Vδ2 mAb and analyzed through a FACS Lyric flow cytometer. **(B) PTA-mediated clustering of γδ T cells.** After stimulation/expansion with PTA/IL-2, cell clustering was monitored under a microscope equipped with a CCD camera.

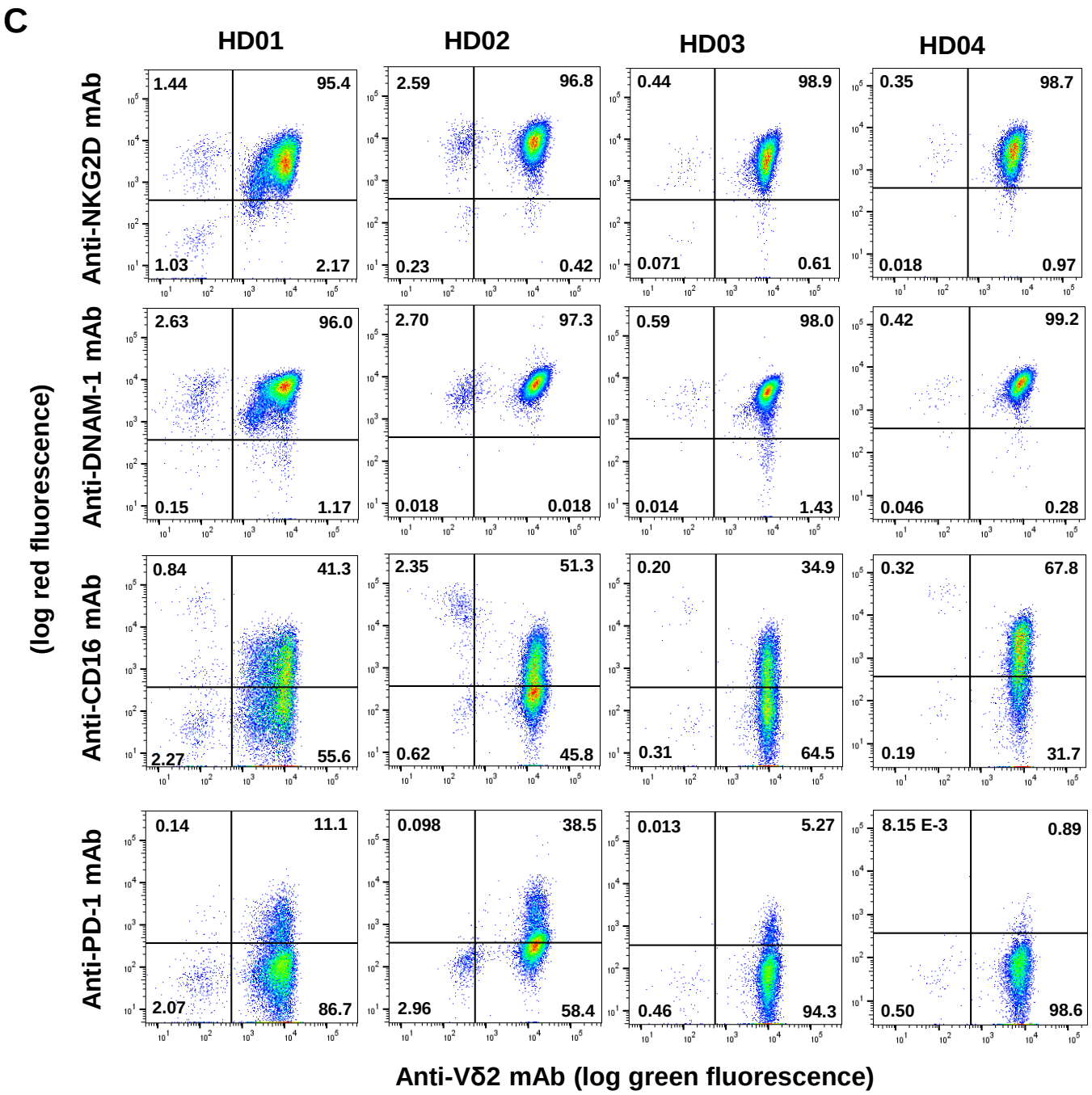

Supplementary Fig. 1. Expansion of γδ T cells from HDs with PTA/IL-2. (C) Flow cytometric analyses of cell surface markers on PTA/IL-2-expanded γδ T cells. After stimulation/expansion with PTA/IL-2 for 11 days, the cells were stained with PE-labeled anti-NKG2D, DNAM-1, CD16, or PD-1 mAb and FITC-labeled anti-Vδ2 mAb and analyzed through a FACS Lyric flow cytometer.

Materials and Methods for Supplementary Fig. 1.

(A) Preparation of PBMC: Peripheral blood samples (14 mL) were collected from HDs using heparin-containing blood collection tubes and transferred into a 15 mL conical tube, which was centrifuged at 2,200 rpm for 10 min at room temperature. After removing the plasma, the cell pellets were diluted with phosphate-buffered saline (PBS) to a volume of 20 mL. The diluted blood was loaded on 20 mL of Ficoll-Paque Plus (Cytiva, Shinjuku-ku, Tokyo, Japan) in a 50 mL conical tube and centrifuged at 1,700 rpm ($600 \times g$) for 30 min at room temperature without acceleration and deceleration. Fluffy layers (lymphocyte fractions) were collected and diluted with 35 mL of PBS in a 50 mL conical tube, which was centrifuged at 2,200 rpm for 10 min at 4 ^{o}C. After the supernatant was discarded, the cell pellets were dispersed with tapping and resuspension in 13 mL of PBS in a 15 mL conical tube. After centrifugation at 1,700 rpm for 5 min at 4 ^{o}C, the cells were resuspended in 7.2 mL of Yssel's medium supplemented with 10% heat-inactivated human AB serum [60] to achieve a maximum cell concentration of 1×10^7 cells/mL. Of the PBMC suspension, 1.2 mL was used for the flow cytometric analysis.

(B) Derivation of γδ T cells: The PBMC suspension (6 mL) was placed in 4 wells of a 24-well plate (Corning Inc., Corning, NY), to which was added 1.5 µL each of 1 mM PTA stock solution (Techno Suzuta Co., Ltd., Heiwa-machi, Nagasaki, Japan) in dimethyl sulfoxide (DMSO) (Nacalai Tesque Inc., Nakagyo-ku, Kyoto, Japan), resulting in a final concentration of 1 µM. The cells were observed under a microscope (Nikon Corp., Minato-ku, Tokyo, Japan) every day during incubation. The plate was incubated at 37 ^{o}C with 5% CO_2 overnight, and IL-2 (Shionogi Pharmaceutical Co., Ltd., Chuo-ku, Osaka, Japan) was added to each well, to obtain a concentration of 100 U/mL, from day 1 to day 9. On day 2, the medium was replaced with fresh Yssel's medium supplemented with 10% heat-inactivated human AB serum to remove any residual PTA/DMSO that might affect the growth in γδ T cells. Whenever the cell density increased to confluency, the cell suspensions were diluted 2-fold with Yssel's medium supplemented with heat-inactivated 10% human AB serum (when culturing in wells) or complete RPMI1640 medium (when culturing in flasks) and split to new wells or flasks until day 9. The γδ T cells were then harvested on day 11. After the flow cytometric analysis, the remaining cells were resuspended in cryo-preservation media, placed at -80 ^{o}C, and stored in liquid nitrogen until used.

(C) Flow cytometric analysis: The cell suspensions, 110 µL each (ca. 1.0×10^5 cells), were dispensed into a 96-well round-bottom plate (Corning Inc.) and centrifuged at 1,700 rpm and 4 ^{o}C for 2 min. After the supernatants were removed, the cell pellets were dispersed by vortexing. The cells were stained with monoclonal antibodies (mAbs), 3 µL each, in 47 µL of PBS/2% fetal calf serum (FCS, Merk, Darmstadt, Hessen, Germany). Immunohistochemical staining was performed using fluorescein isothiocyanate (FITC)-conjugated anti-TCR Vδ2 mAb (Beckman Coulter Inc., Pasadena, CA); phycoerythrin (PE)-conjugated anti-CD3 mAb (Thermo Fisher Scientific Inc.), and anti-NKG2D, anti-DNAM-1, and anti-CD16 mAbs (BioLegend Japan, Bunkyo-ku, Tokyo, Japan), unlabeled anti-PD-1 mAb (Medical & Biological Laboratories Co., Ltd., Minato-ku, Tokyo, Japan); and R-PE-conjugated anti-mouse immunoglobulin Ab (Agilent Technologies, Santa Clara, CA). After the plate was incubated on ice for 15 min, the cells were centrifuged with 100 µL of PBS at 1,700 rpm for 2 min at 4 ^{o}C. After the supernatants were removed, the cell pellets were dispersed by vortexing. The cells were, subsequently, washed three times with 200 µL of PBS via centrifugation at 1,700 rpm for 2 min at 4 ^{o}C, and they were resuspended in 200 µL of 1% paraformaldehyde in PBS. The cell suspensions were passed through a mesh filter membrane and analyzed using a FACS Lyric flow cytometer (Becton Dickenson, Franklin, Lakes, NJ). The cell population was visualized with FlowJo ver. 10.8.1 (FlowJo LLC, Ash-land, OR).

Results for Supplementary Fig. 1. Expansion of γδ T cells from HDs with PTA/IL-2.

(A) Flow cytometric analyses of PTA/IL-2-mediated expansion of γδ T cells derived from HDs. As HDs,12 males and 4 females were enrolled in this study. The median age at the time of blood sampling was 34 years (range, 27–58 years). PBMC were isolated through a standard Ficoll density centrifugation procedure, of which 4 representative results of flow cytometric analyses are depicted in the upper panels. The proportions of Vδ2-expressing γδ T cells (termed γδ T cells hereafter) in PBMC on day 0 were 1.06%, 4.96%, 5.39%, and 28.8% for HD01–04, respectively, and the median proportion of γδ T cells in $CD3^+$ lymphocyte fractions was 3.82% (range, 0.56%–39.4%).

After the PBMCs were stimulated with PTA, a nitrogen-containing bisphosphonate prodrug, and IL-2 for 11 days, the proportions of γδ T cells increased to 95.7%, 96.9%, 99.4%, and 99.6% for HD01–04, respectively, as shown in the lower panels. The median proportion of γδ T cells in $CD3^+$ lymphocyte fractions increased to 99.19%, with a range of 94.56%-99.92%. The median number of γδ T cells (per mL of blood) before and after expansion was 6.3×10^4 (range: 6×10^3–4.75×10^5) and 1.04×10^8 (range: 4×10^6–2.03×10^8), respectively, and the median expansion rate of the γδ T cells was 1091-fold (range: 415–4835). Consistent with our previous results, a large number of highly purified γδ T cells were obtained using the PTA/IL-2 stimulation/expansion system [50] when the proportion of γδ T cells in the $CD3^+$ lymphocyte fractions was well above 1%.

(B) PTA-mediated clustering of γδ T cells. Microscopic analyses revealed that the cells started to form clusters 3 to 5 days following PTA/IL-2 stimulation.

(C) Flow cytometric analyses of cell surface markers on PTA/IL-2-expanded γδ T cells. Since γδ T cells are categorized into both innate immune cells and adaptive immune cells, we next examined the cell surface expression of NK receptors [62-67], such as natural killer group 2 member D (NKG2D, CD314), DNAX accessory molecule-1 (DNAM-1, CD226), and CD16 (FcγRIIIA), whose expressions are inexorably linked to NK cells. Based on the flow cytometric analyses, essentially all of the PTA/IL-2-expanded γδ T cells expressed NKG2D and DNAM-1, as shown in Supplementary Figure 1C. The median proportions of NKG2D and DNAM-1 in the γδ T cells were 98.93% (range: 96.04%–99.96%) and 98.97% (range: 96.5%–99.99%), respectively. On the contrary, the majority of γδ T cells failed to express a high level of FasL (CD95L) and TRAIL (human TNF-related apoptosis-inducing ligand) (data not shown). The median proportions of FasL and TRAIL in γδ T cells were 0.09% (range: 0.03%–4.78%) and 0.19% (range: 0.03%–5.27%), respectively. γδ T cells expressed CD16 to different degrees depending on the individual, and the median proportion of CD16-expressing γδ T cells was 38.9% (range: 7.5%–70.9%). It has been reported that programmed death-1 $(PD\text{-}1)^+$ γδ T cells could produce a significantly higher level of IL-2 in response to (*E*)-4-hydroxy-3-methylbut-2-enyl diphosphate (HMBPP) than $PD\text{-}1^-$ γδ T cells did, and the expression of PD-1 on γδ T cells generally attained the maximum within 3 days after stimulation with pyrophosphomonoester antigens and gradually declined thereafter [68-69]. We, thus, examined the level of PD-1 expression in γδ T cells after stimulation/expansion with PTA/IL-2. It is of note that only a small portion of γδ T cells expressed a low level of PD-1, and the median proportion of PD-1 in γδ T cells was 11.35% (range: 0.9%–59.4%).

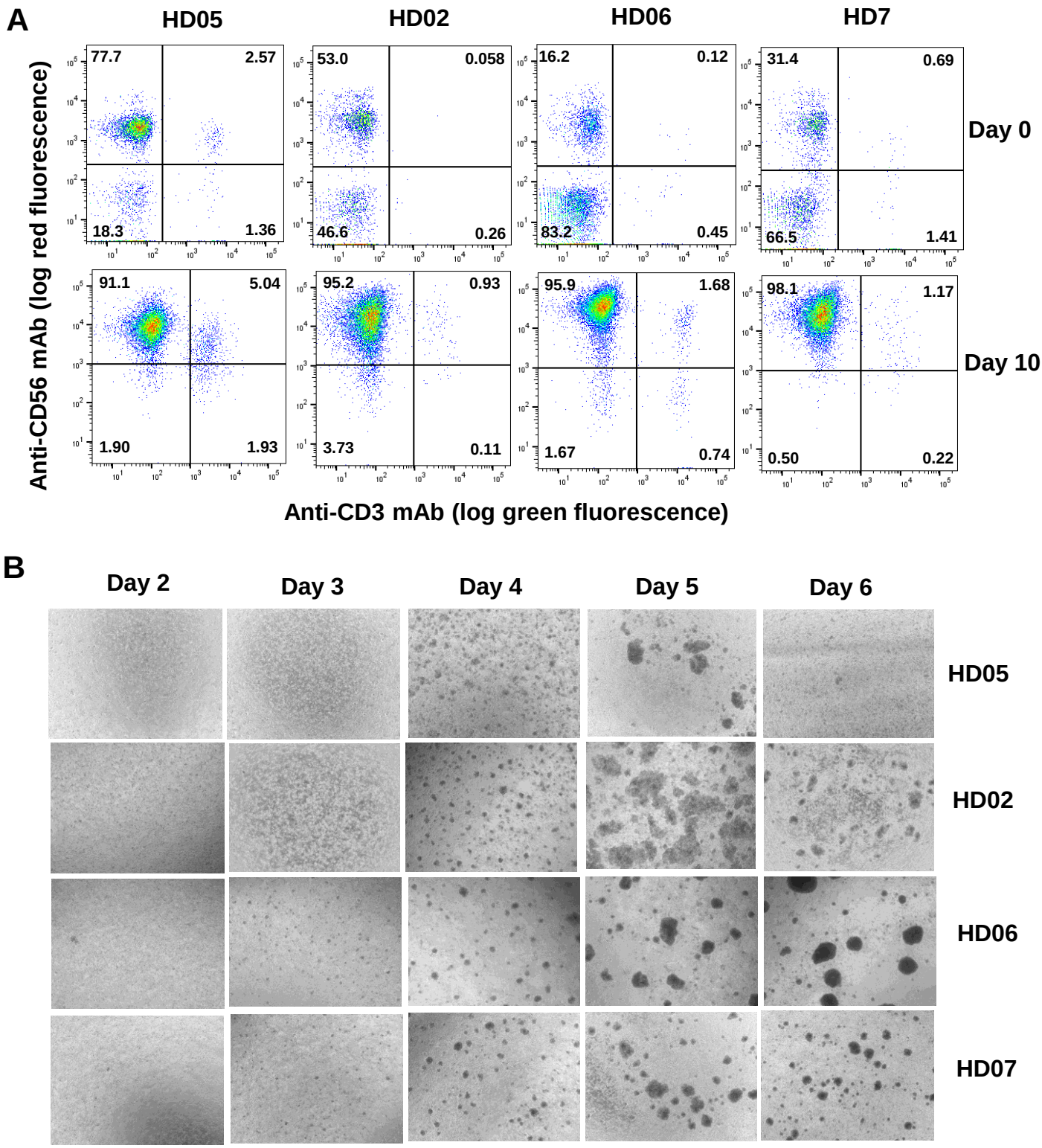

Supplementary Fig. 2. Expansion of NK cells from HDs with IL-2/IL-18. (A) Flow cytometric analyses of IL-2IL-18-mediated expansion of NK cells derived from HDs. Before and after expansion for 10 days with IL-2/IL-18, the cells were stained with PE-labeled anti-CD56 mAb and FITC-labeled anti-CD3 mAb and analyzed through a FACS Lyric flow cytometer. **(B) IL-2/IL-18-mediated clustering of NK cells.** After stimulation with IL-2/Il-18, the cell clustering was monitored under a microscope equipped with a CCD camera.

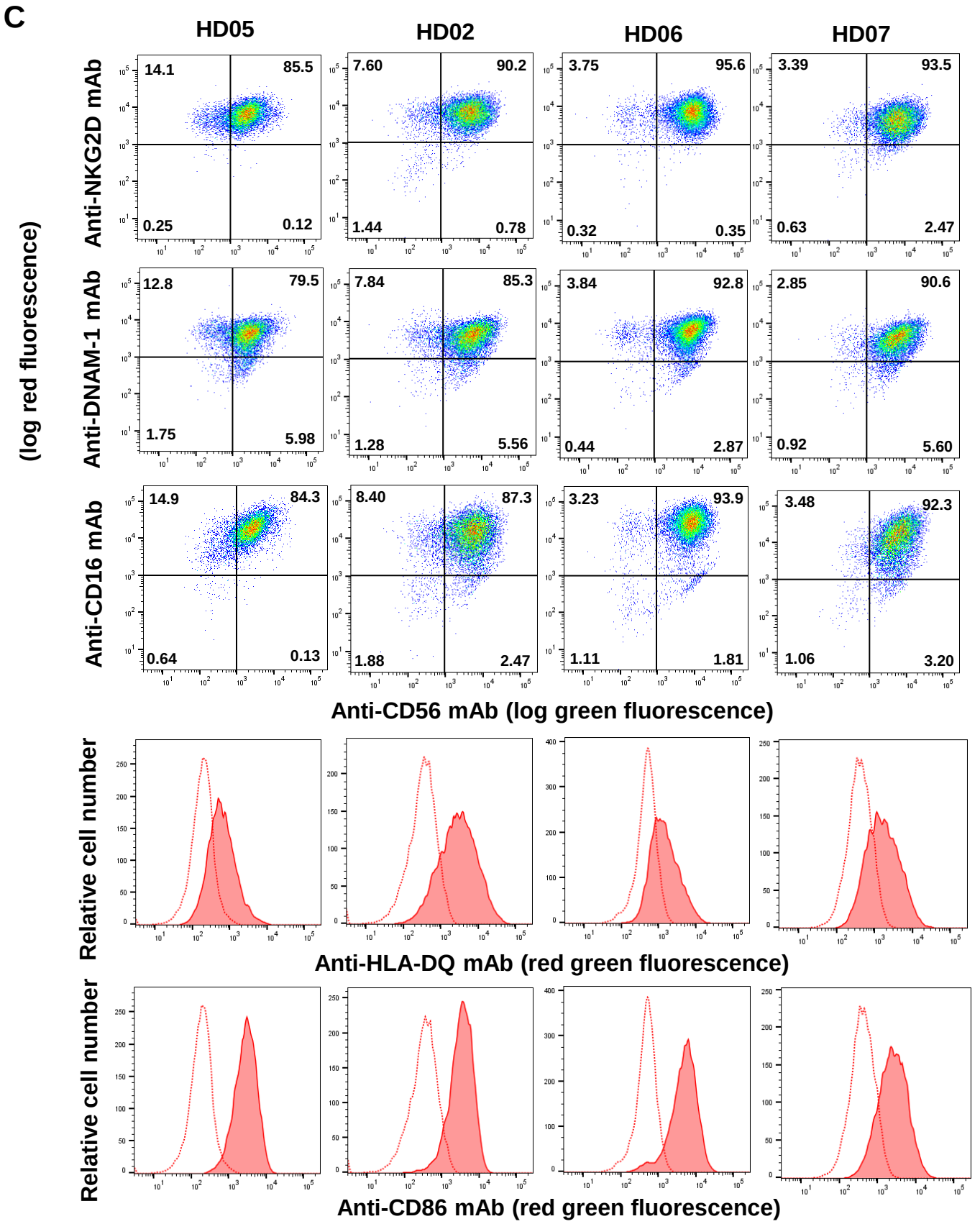

Supplementary Fig. 2. Expansion of NK cells from HDs with IL-2/IL-18. (C) Flow cytometric analyses of cell surface markers on IL-2/IL-18-expanded NK cells. After expansion with IL-2/IL-18 for 10 days, the cells were stained with PE-labeled anti-NKG2D, DNAM-1, CD16, HLA-DQ, or CD86 mAb and FITC-labeled anti-CD56 mAb and analyzed through a FACS Lyric flow cytometer.

Materials and Methods for Supplementary Fig. 2.

(A) Derivation of NK cells: PBMCs were prepared as described in Supplementary Fig. 1. After 6 mL of the PBMC suspension, in a 15 mL conical tube, was centrifuged at 1,700 rpm at 4 °C for 5 min, the supernatant was removed and the cell pellets were dispersed by tapping and resus-pended in 200 μL of PBS/0.5% BSA/2 mM EDTA. To the PBMC suspension was added 100 μL of anti-CD3 MACSBeads (Miltenyi Biotech, Bergisch-Gladbach, Germany) and the tube was placed at 4 °C. After 15 min, 10 mL of PBS/0.5% BSA/2 mM EDTA was added to the cell suspension. The tube was then centrifuged at 300 × g for 10 min at 4 °C and the supernatant was removed. The cell pellets and beads were dispersed by tapping and resuspended in 1 mL of PBS/0.5% BSA/2 mM EDTA. The cell/bead suspension was loaded onto an LD Column (Miltenyi Biotech), which had been attached to a magnet holder and equilibrated with 2 mL of PBS/0.5% BSA/2 mM EDTA. The $CD3^-$ cells were eluted with 2 × 1 mL of PBS/0.5% BSA/2 mM EDTA into a 15 mL conical tube, to which was added 6 mL of Yssel's medium supplemented with 10% human AB serum. After the tube was centrifuged at 1,700 rpm for 5 min at 4 °C, the $CD3^-$ cells were resuspended in 5 mL of Yssel's medium supplemented with 10% heat-inactivated human AB serum. Of the cell suspension, 1.5 mL was used for the flow cytometric analysis. The rest of the cell suspension was centrifuged at 1,700 rpm for 5 min at 4 °C. After the supernatant was removed, the cell pellets were dispersed by tapping and resuspended in 3 mL of Yssel's medium supplemented with 10% heat-inactivated human AB serum. The PBMC suspension (3 mL) was placed in 2 wells of a 24-well plate, to which was added 100 IU/mL IL-2 and 100 ng/mL recombinant human IL-18 (Techno Suzuta Co., Ltd), expressed in E. coli from day 0 to day 8. Cell passages were conducted based on cell confluency until day 8. Then, the NK cells were harvested on day 10 and analyzed using flow cytometry. The NK cells were placed at -80 °C and then stored in a liquid nitrogen tank until used.

(B) Flow cytometric analysis: Immunohistochemical staining was performed using FITC-conjugated anti-CD3 mAb (Thermo Fisher Scientific Inc.) and anti-CD56 mAb (BioLegend, San Diego, CA); and phycoerythrin (PE)-conjugated anti-CD56, anti-NKG2D, anti-DNAM-1, anti-CD16, anti-HLA-DQ, and anti-CD86 mAbs (BioLegend). The stained cells were analyzed using a FACS Lyric flow cytometer (Becton Dickenson) and the cell population was visualized with FlowJo ver. 10.8.1 (FlowJo LLC) as described in Supplementary Fig. 1.

Results for Supplementary Fig. 2. Expansion of NK cells from HDs with IL-2/IL-18.

(A) Flow cytometric analyses of IL-2IL-18-mediated expansion of NK cells derived from HDs.

PBMC were prepared from 10 HDs as described in Supplementary Fig. 1, then $CD3^+$ cells were depleted using anti-CD3 mAb-coated beads. Four representative results of flow cytometric analyses of the $CD3^-$ depleted PBMCs (HD02, 05–07) are shown in the upper panels. The proportions of $CD3^-CD56^+$ NK cells after treatment with anti-CD3 mAb beads were 77.7%, 53.0%, 16.2%, and 31.4%, respectively, and the median proportion of NK cell fractions after CD3 removal was 49.9% (range: 31.4% – 92.3%).

After the $CD3^-$ PBMCs were stimulated/expanded with IL-2 and IL-18 for 10 days. The proportion of NK cells increased to 91.1%, 95.2%, 95.9%, and 98.1%, for HD02, 05–07, respectively as depicted in the lower panels. The median proportion of NK cells after expansion was 95.45%, with a range of 71.4%–98.4%. The median number of NK cells (per mL of blood) before and after expansion was 2.04×10^5 (range: 4.5×10^4–9.84×10^5) and 5×10^6 (range: 4×10^5–1.6×10^7), respectively. The median expansion rate of the NK cells was 40-fold (range: 1.1–74.5). We, thus, obtained highly purified NK cells using the IL-2/IL-18 expansion system. The expansion rate of the NK cells was, however, significantly low compared to that of γδ T cells.

(B) IL-2/IL-18-mediated clustering of NK cells. Microscopic analyses revealed that cells started to form clusters 4 to 5 days after stimulation with IL-2/IL-18.

(C) Flow cytometric analyses of cell surface markers on IL-2/IL-18-expanded NK cells. Based on flow cytometric analyses of the cell surface markers after IL-2/IL-18 stimulation, essentially all of the expanded NK cells expressed high levels of NKG2D, DNAM-1, and CD16, as shown in the upper bivariate histograms. The median proportions of NKG2D and DNAM-1 in the NK cells were 99.65% (range: 94.98%–99.86%) and 94.03% (range: 77.4%–99.04%), respectively. It is noteworthy that essentially all NK cells expressed a high level of CD16, which is in contrast to γδ T cells; in fact, the median proportion of $CD16^+$ NK cells was 96.76% (range: 59.48%–99.85%).

It was previously reported that NK cells express cell surface molecules, typically expressed on antigen-presenting cells, in response to IL-2/IL-18. In addition, the cytolytic functions of NK cells are intricately controlled by activating and inhibiting receptors, including human leukocyte antigen (HLA) molecules [70] and cluster of differentiation 86 (CD86, B7-2) [71]. We, thus, examined the expressions of HLA-DQ and CD86 on the NK cells after stimulation/expansion with IL-2/IL-18. As shown in the lower univariate histograms, more than half of the NK cells expressed high levels of HLA-DQ and CD86; the median proportions of $HLA\text{-}DQ^+$ and $CD86^+$ cells in the IL-2/IL-18-stimulated NK cells was 63.78% (range: 27.89%–93.91%) and 92.25% (range: 75.72%–93.94%), respectively.

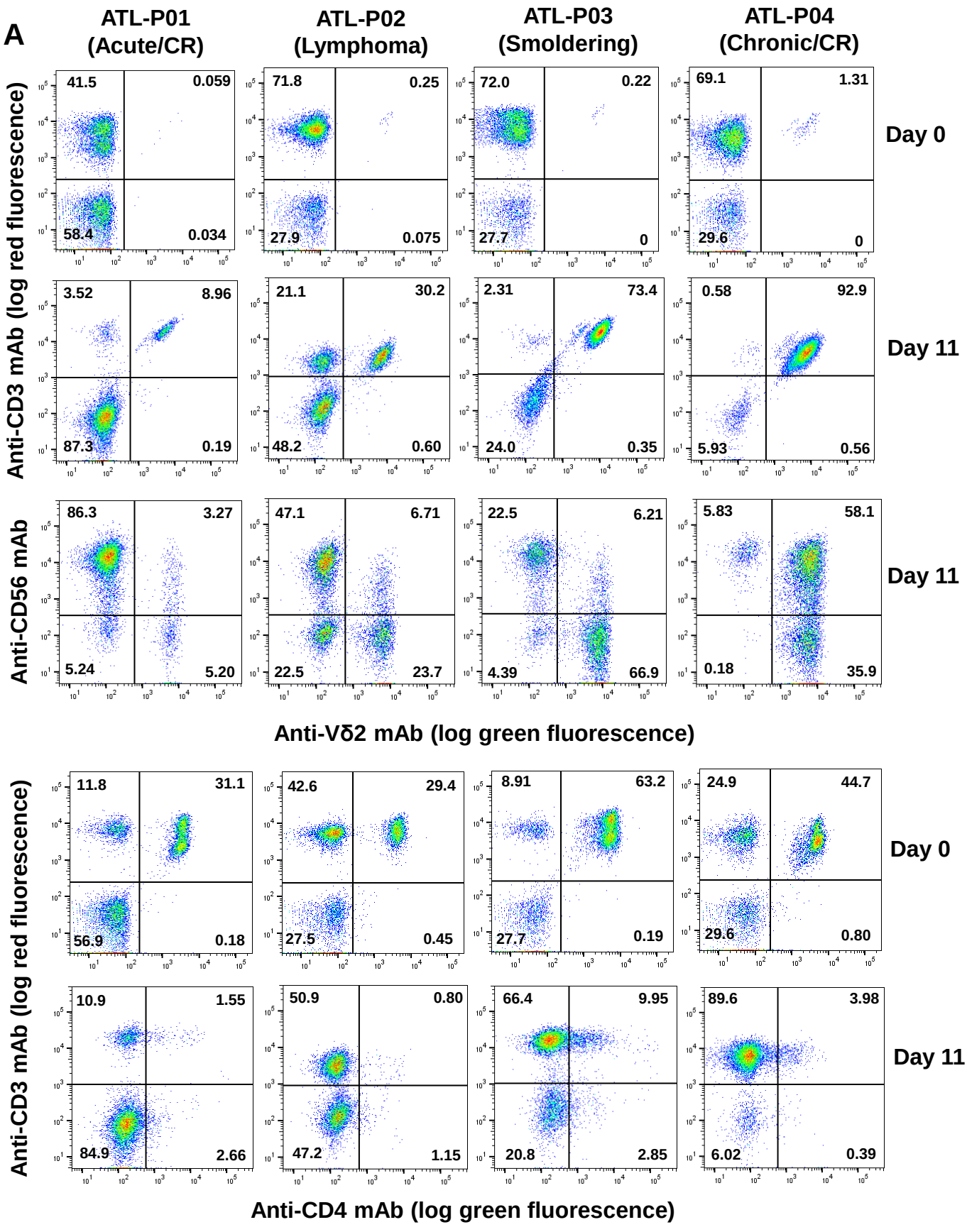
A
ATL-P01 (Acute/CR)
ATL-P02 (Lymphoma)
ATL-P03 (Smoldering)
ATL-P04 (Chronic/CR)
Day 0
Day 11
Day 11
Anti-CD3 mAb (log red fluorescence)
Anti-CD56 mAb
Anti-Vδ2 mAb (log green fluorescence)
41.5
0.059
58.4
0.034
71.8
0.25
27.9
0.075
72.0
0.22
27.7
0
69.1
1.31
29.6
0
3.52
8.96
87.3
0.19
21.1
30.2
48.2
0.60
2.31
73.4
24.0
0.35
0.58
92.9
5.93
0.56
86.3
3.27
5.24
5.20
47.1
6.71
22.5
23.7
22.5
6.21
4.39
66.9
5.83
58.1
0.18
35.9
Day 0
Day 11
Anti-CD3 mAb (log red fluorescence)
Anti-CD4 mAb (log green fluorescence)
11.8
31.1
56.9
0.18
42.6
29.4
27.5
0.45
8.91
63.2
27.7
0.19
24.9
44.7
29.6
0.80
10.9
1.55
84.9
2.66
50.9
0.80
47.2
1.15
66.4
9.95
20.8
2.85
89.6
3.98
6.02
0.39

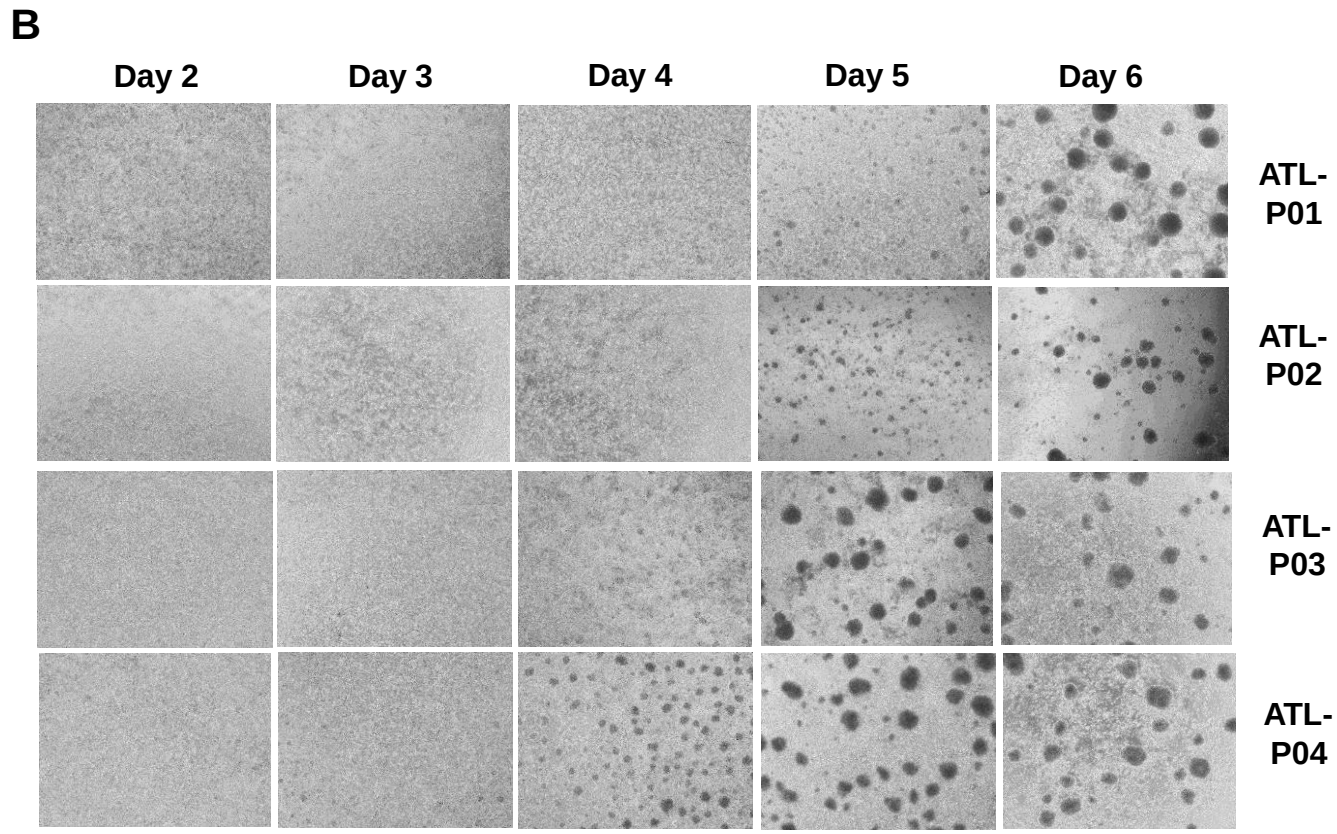

Supplementary Fig. 3. Expansion with PTA/IL-2/Il-18 of γδ T cells and NK cells derived from ATL patients. (A) Flow cytometric analyses of PTA/IL-2/IL-18-mediated expansion of γδ T cells and NK cells derived from ATL patients. PBMCs were purified from peripheral blood derived from ATL patients and stimulated/expanded with PTA/IL-2/IL-18, which were analyzed through flow cytometry. **(B) PTA/IL-2/IL-18-mediated clustering of γδ and NK cells.** After stimulation with PTA/IL-2/IL-18, the cell clustering was monitored under a microscope equipped with a CCD camera.

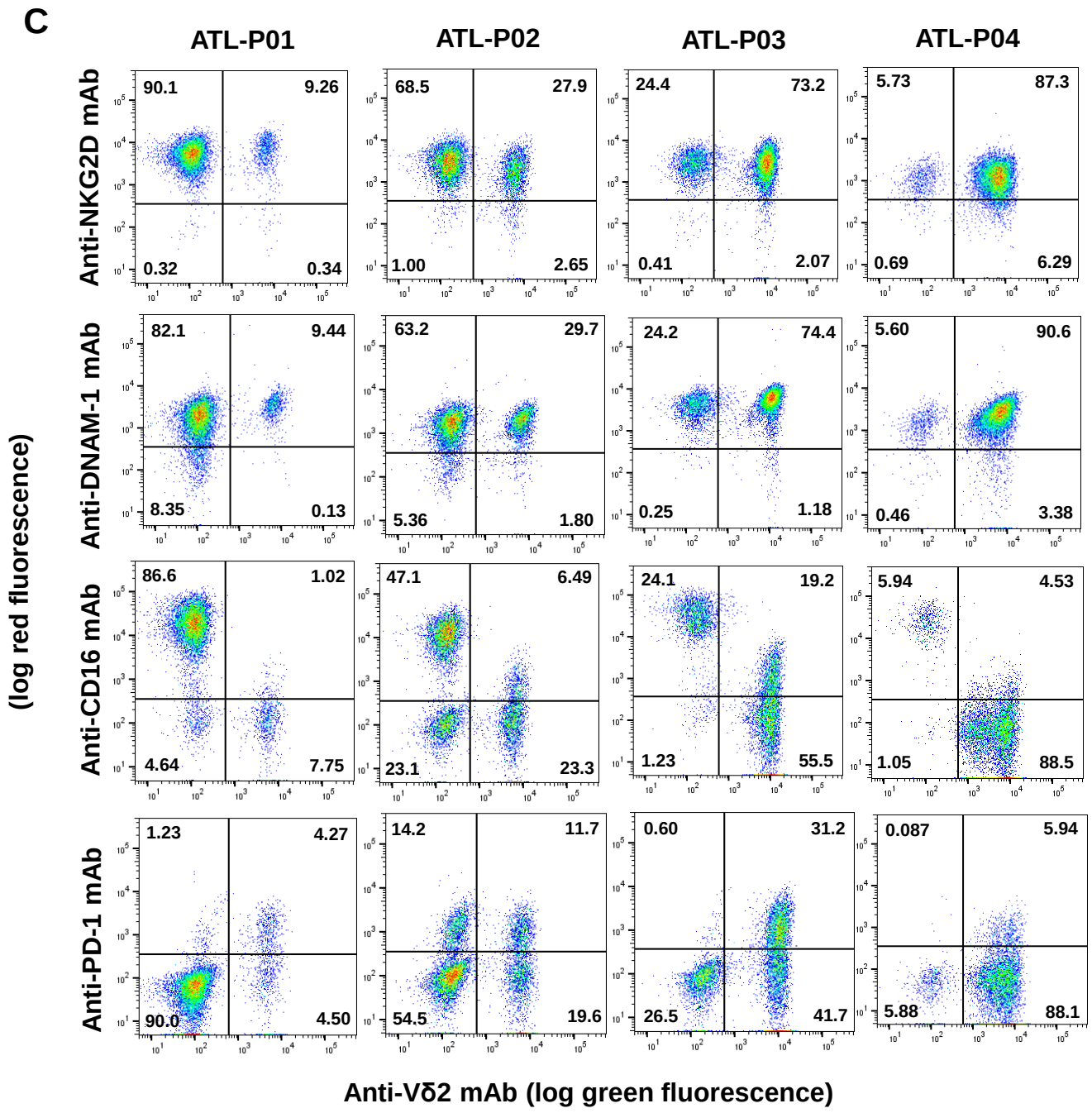

Supplementary Fig. 3. Expansion with PTA/IL-2/Il-18 of γδ T cells and NK cells derived from ATL patients. (C) Flow cytometric analyses of PTA/IL-2/IL-18-mediated expansion of γδ T cells and NK cells derived from ATL patients. After stimulation/expansion of PBMCs derived from ATL patients with PTA/IL-2/IL-18, the cells were stained with PE-conjugated anti-NKG2D, anti-DNAM-1, or anti-CD16 mAb and FITC-conjugated anti-Vδ2 mAb, or anti-PD-1 plus RPE-conjugated anti-mouse Ig ab plus FITC-conjugated anti-Vδ2 mAb and analyzed through a FACS Lyric flow cytometer.

Materials and Methods for Supplementary Fig. 3.

(A) Derivation of γδ T cells and NK cells from PBMC obtained from ATL patients: PBMC were purified from ATL patients-derived PBMC as described in Supplementary Fig. 1, from which γδ T cells and NK cells were prepared as described in Supplementary Figs. 1 and 2.

(B) Flow cytometric analysis: Immunohistochemical staining was performed using FITC-conjugated anti-TCR Vδ2 mAb (Beckman Coulter Inc.) and anti-CD4 mAbs (FUJIFILM Wako Pure Chemical Corp., Chuo-ku, Osaka, Japan); PE-conjugated anti-CD3 mAb (Thermo Fisher Scientific Inc.), and anti-CD56, anti-NKG2D, anti-DNAM-1, and anti-CD16 mAbs (BioLegend), unlabeled anti-PD-1 mAb (Medical & Biological Laboratories Co., Ltd); and R-PE-conjugated anti-mouse immunoglobulin Ab (Agilent Technologies). The stained cells were analyzed using a FACS Lyric flow cytometer (Becton Dickenson) and the cell population was visualized with FlowJo ver. 10.8.1 (FlowJo LLC) as described in Supplementary Fig. 1.

Results for Supplementary Fig. 3. Expansion with PTA/IL-2/Il-18 of γδ T cells and NK cells derived from ATL patients.

(A) Flow cytometric analyses of PTA/IL-2/IL-18-mediated expansion of γδ T cells and NK cells derived from ATL patients. **:** PBMC derived from 55 ATL patients (initial 25 patients plus additional 30 patients) were stimulated/expanded with PTA/IL-2/IL-18, of which 4 representative flow cytometry diagrams (ATL-P01–04) are depicted in the upper panels. The median proportion of γδ T cells in $CD3^+$ lymphocyte fractions before expansion was 0.29% (range: 0.0%–7.41%). After stimulation/expansion with PTA/IL-2/IL-18 for 11 days, the median proportion of γδ T cells in $CD3^+$ lymphocyte fractions increased to 87.99% (range: 0.55%–99.38%). The median number of γδ T cells (per mL of blood) before and after expansion was 4.2×10^3 (range: $0.0–6.6 \times 10^4$) and 3.5×10^6 (range: $2 \times 10^3–1.75 \times 10^8$), respectively. The median expansion rate of the γδ T cells was 1998-fold (range: 4–32844). It is intriguing that $CD3^-CD56^+$ cells (corresponding to NK cells) were increased when the proportion of γδ T cells were low on day 11.

Since ATL is a mature peripheral $CD3^+CD4^+$ T-cell malignancy, we examined the proportion of $CD4^+$ T cells in $CD3^+$ lymphocyte fractions. Four representative flow cytometry diagrams are shown in the lower panels. The median proportions of $CD4^+$ T cells in $CD3^+$ lymphocyte fractions before and after expansion with PTA/IL-2/IL-18 were 72.49% (range: 30.33%–99.5%) and 6.67% (range: 0.76%–99.76%), respectively. The proportion of $CD4^+$ T cells in $CD3^+$ lymphocyte fractions was greatly reduced in most cases after the expansion with for 11 days, suggesting that a combination of γδ T cells and NK cells exhibited cellular cytotoxicity against HTLV-1-infected $CD4^+$ T cells.

(B) PTA/IL-2/IL-18-mediated clustering of γδ and NK cells. : A microscopic analysis revealed that the cells started to form clusters 3 to 6 days after stimulation.

(C) Flow cytometric analyses of PTA/IL-2/IL-18-mediated expansion of γδ T cells and NK cells derived from ATL patients. After expansion with PTA/IL-2/IL-18, essentially all the expanded γδ T cells expressed NKG2D and DNAM-1. The median proportions of NKG2D and DNAM-1 in the γδ T cells were 97.40% (range: 82.81% – 99.9%) and 98.79% (range: 92.86%–99.91%), respectively. The γδ T cells expressed CD16 to different degrees; in fact, the median proportion of CD16 in the γδ T cells was 17.7% (range: 0.98%–89.94%). In addition, the γδ T cells expressed, to different degrees, a low level of PD-1, and the median proportion of PD-1 in the γδ T cells was 29.87% (range: 2.76%–57.93%).

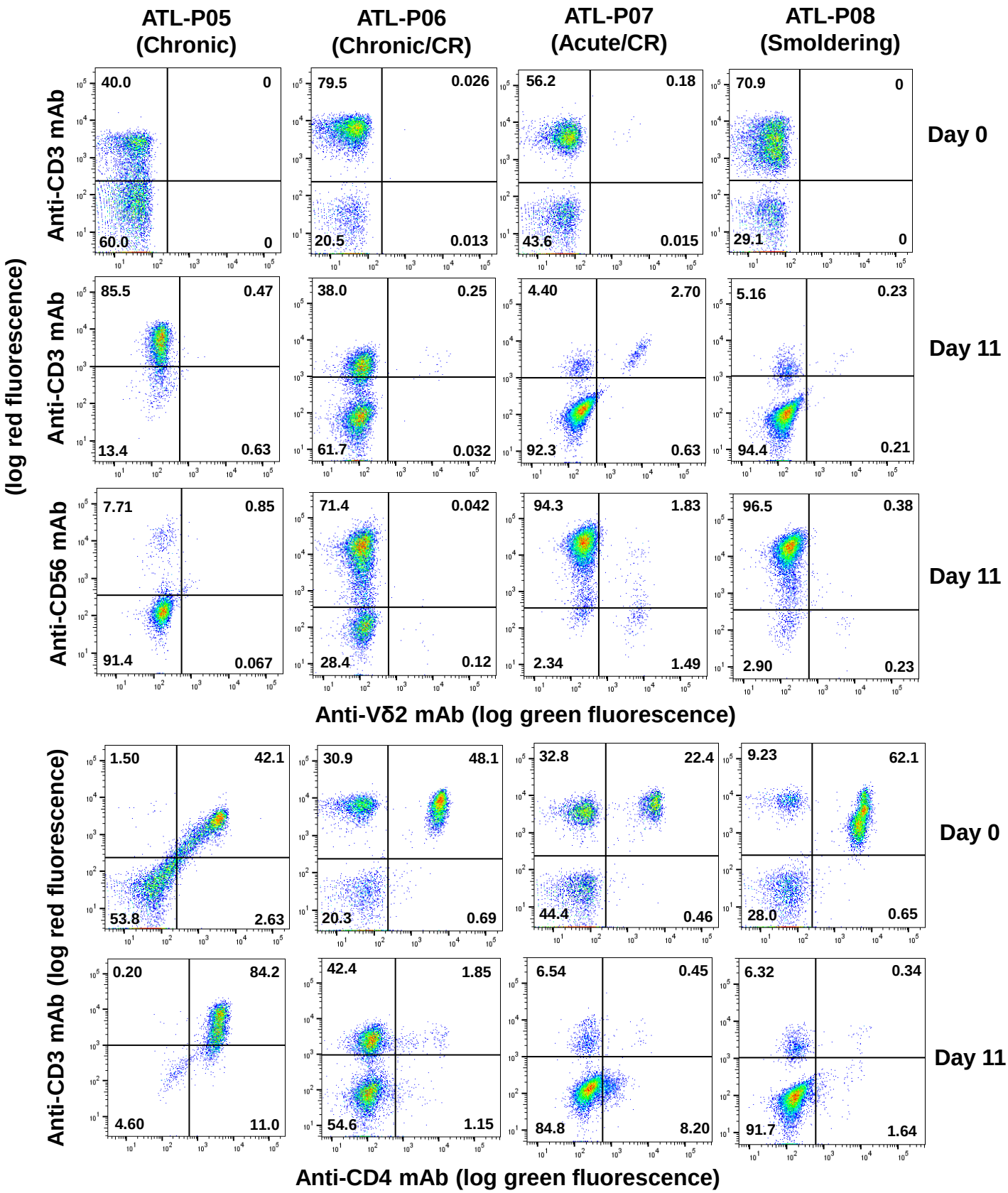

Supplementary Fig. 4. Effect of PTA/IL-2/Il-18 on the expansion of γδ T cells derived from ATL patients. Flow cytometric analyses of PTA/IL-2/IL-18-mediated expansion of γδ T cells and NK cells derived from ATL patients. PBMCs were purified from peripheral blood derived from ATL patients and stimulated/expanded with PTA/IL-2/IL-18, which were analyzed through flow cytometry.

Materials and Methods for Supplementary Fig. 4.

(A) Derivation of γδ T cells from PBMC obtained from ATL patients: PBMC were purified from ATL patients-derived PBMC as described in Supplementary Fig. 1. The PBMC suspension (6 mL) was placed in 4 wells of a 24-well plate (Corning Inc., Corning, NY), to which was added 1.5 μL each of 1 mM PTA stock solution (Techno Suzuta Co., Ltd.) in DMSO (Nacalai Tesque) to give a final concentration of 1 μM and IL-18 (Techno Suzuta Co., Ltd.) at a final concentration of 100 ng/mL. The cells were observed under a microscope (Nikon Corp., Minato-ku, Tokyo, Japan) every day during incubation. The plate was incubated at 37 ^{o}C with 5% CO_2 overnight, and IL-2 (Shionogi Pharmaceutical Co., Ltd.) and IL-18 (Techno Suzuta Co., Ltd.) were added to each well, to obtain a concentration of 100 U/mL and 100 ng/mL, respectively, from day 1 to day 9. On day 2, the medium was replaced with fresh Yssel's medium supplemented with 10% heat-inactivated human AB serum to remove any residual PTA/DMSO that might affect the growth in γδ T cells. Whenever the cell density increased to confluency, the cell suspensions were diluted 2-fold with Yssel's medium supplemented with heat-inactivated 10% human AB serum (when culturing in wells) or complete RPMI1640 medium (when culturing in flasks) and split to new wells or flasks until day 9. The γδ T cells were then harvested on day 11. After the flow cytometric analysis, the remaining cells were resuspended in cryo-preservation media, placed at -80 ^{o}C, and stored in liquid nitrogen until used.

(B) Flow cytometric analysis: Immuno-histochemical staining was performed using FITC-conjugated anti-TCR Vδ2 mAb (Beckman Coulter Inc.) and anti-CD4 mAb (FUJIFILM Wako Pure Chemical Corp.), and PE-conjugated anti-CD3 mAb (Thermo Fisher Scientific Inc.) and anti-CD56 mAb (BioLegend) and analyzed using a FACS Lyric flow cytometer (Becton Dickenson). The stained cells were analyzed using a FACS Lyric flow cytometer (Becton Dickenson) and the cell population was visualized with FlowJo ver. 10.8.1 (FlowJo LLC) as described in Supplementary Fig. 1.

Results for Supplementary Fig. 4. Effect of PTA/IL-2/Il-18 on the expansion of γδ T cells derived from ATL patients. Flow cytometric analyses of PTA/IL-2/IL-18-mediated expansion of γδ T cells and NK cells derived from ATL patients. In some ATL patients, the proportions of γδ T cells were extremely low before expansion. Flow cytometric diagrams of 4 representative ATL patients (ATL-P05–08), with extremely low proportions of γδ T cells are shown, in which γδ T cells occupied only 0%–0.18% of lymphocyte fractions. When the PBMCs were stimulated with PTA/IL-2/IL-18, only a marginal level of γδ T cell expansion was observed. Instead, in three out of four patients (ATL-P06–08), the $CD56^{+}CD3^{-}$ populations (corresponding to NK cells) increased. In the case of ATL-P05, both γδ T cells and NK cells failed to proliferate well in response to PTA/IL-2/IL-18. Among the 55 ATL patients, 3 did not respond at all to PTA/IL-2/IL-18, in which the populations of γδ T cells in $CD3^{+}$ T cells from their peripheral blood were less than 0.1% without exception. In fact, the initial frequency of γδ T cells in the $CD3^{+}$ lymphocyte fractions was less than 0.1% in 16 of 54 ATL patients (one particular case with $CD3^{-}$ HTLV-1-infected cells was excluded), whereas such a low frequency of γδ T cells was not observed in HDs. Conversely, the initial frequencies of γδ T cells in $CD3^{+}$ lymphocyte fractions were more than 1% in 12 of 54 ATL patients, whereas such conditions were met in 14 out of 16 HDs. In addition, the proportion of $CD3^{dim}CD4^{+}$ T cells in lymphocyte fractions was greatly reduced in most cases after the expansion with PTA/IL-2/IL-18 for 11 days, suggesting that a combination of γδ T cells and NK cells exhibited cellular cytotoxicity against HTLV-1-infected $CD3^{dim}CD4^{+}$ T cells.

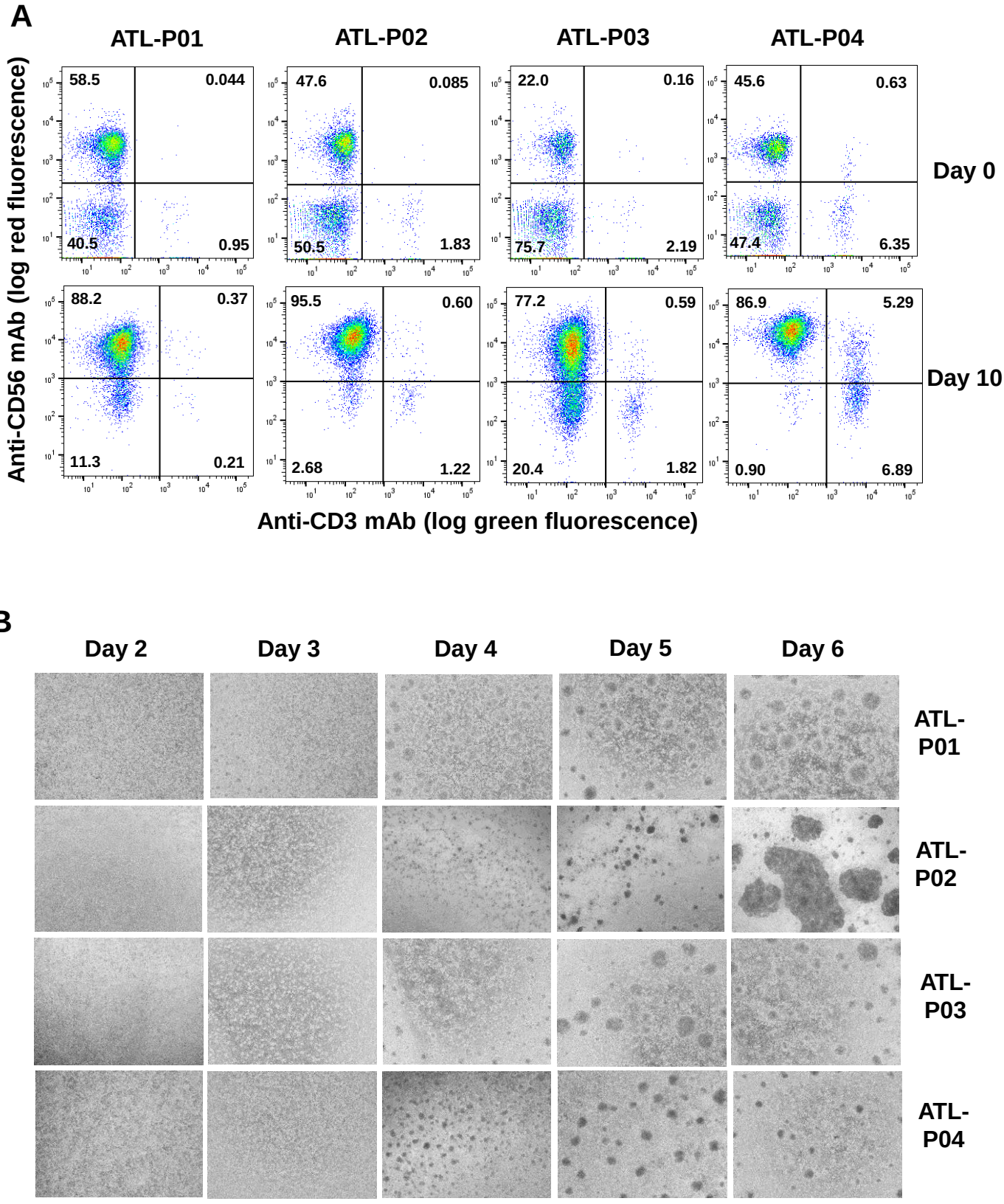
A
ATL-P01
ATL-P02
ATL-P03
ATL-P04
Day 0
Day 10
58.5
0.044
40.5
0.95
47.6
0.085
50.5
1.83
22.0
0.16
75.7
2.19
45.6
0.63
47.4
6.35
88.2
0.37
11.3
0.21
95.5
0.60
2.68
1.22
77.2
0.59
20.4
1.82
86.9
5.29
0.90
6.89
Anti-CD56 mAb (log red fluorescence)
Anti-CD3 mAb (log green fluorescence)
B
Day 2
Day 3
Day 4
Day 5
Day 6
ATL-P01
ATL-P02
ATL-P03
ATL-P04

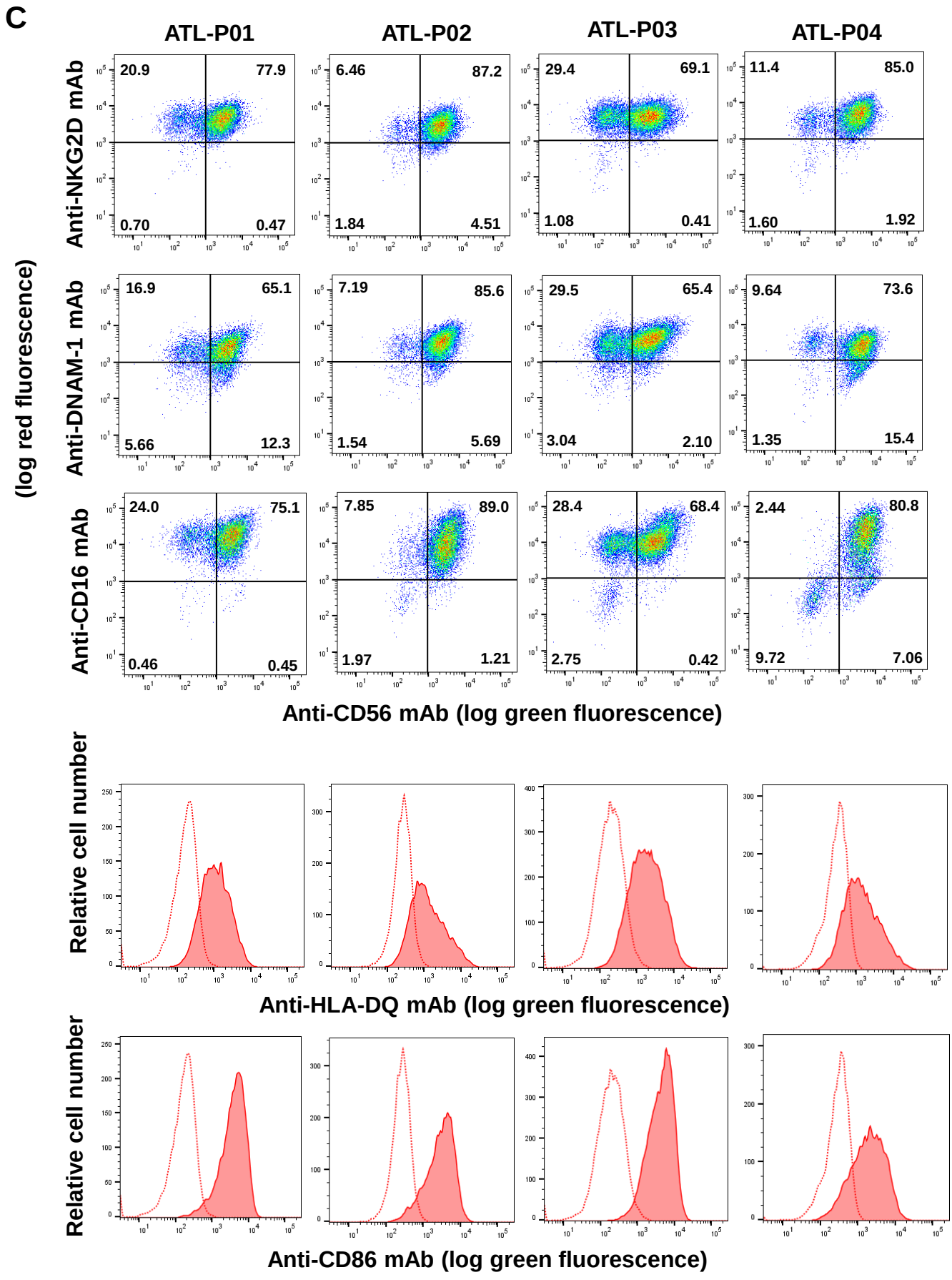
C
ATL-P01
ATL-P02
ATL-P03
ATL-P04
Anti-NKG2D mAb
Anti-DNAM-1 mAb
Anti-CD16 mAb
(log red fluorescence)
20.9
77.9
0.70
0.47
6.46
87.2
1.84
4.51
29.4
69.1
1.08
0.41
11.4
85.0
1.60
1.92
16.9
65.1
5.66
12.3
7.19
85.6
1.54
5.69
29.5
65.4
3.04
2.10
9.64
73.6
1.35
15.4
24.0
75.1
0.46
0.45
7.85
89.0
1.97
1.21
28.4
68.4
2.75
0.42
2.44
80.8
9.72
7.06
Anti-CD56 mAb (log green fluorescence)
Relative cell number
Anti-HLA-DQ mAb (log green fluorescence)
Relative cell number
Anti-CD86 mAb (log green fluorescence)

Supplementary Fig. 5. Expansion with IL-2/IL-18 of NK cells from ATL patients. (A) Flow cytometric analyses of IL-2/IL-18-mediated expansion of NK cells derived from ATL patients. Before and after expansion with IL-2/IL-18, the cells were stained with PE-labeled anti-CD56 mAb and FITC-labeled anti-CD3 mAb and analyzed through a FACS Lyric flow cytometer. **(B) IL-2/IL-18-mediated clustering of NK cells.** After stimulation with IL-2/IL-18, the cell clustering was monitored under a microscope equipped with a CCD camera. **(C) Flow cytometric analysis of cell surface markers on IL-2/IL-18-expanded NK cells.** After expansion with IL-2/IL-18 for 10 days, the cells were stained with PE-labeled anti-NKG2D, DNAM-1, CD16, HLA-DQ, or CD86 mAb and FITC-labeled anti-CD56 mAb and analyzed through a FACS Lyric flow cytometer.

Materials and Methods for Supplementary Fig. 5.

(A) Derivation of NK cells from PBMC obtained from ATL patients: PBMC were purified from ATL patients-derived PBMC as described in Supplementary Fig. 1, from which NK cells were prepared as described in Supplementary Fig. 2.

(B) Flow cytometric analysis: Immunohistochemical staining was performed using FITC-conjugated anti-CD3 mAb (Thermo Fisher Scientific Inc.) and anti-CD56 mAb (BioLegend); and PE-conjugated anti-CD56, anti-NKG2D, anti-DNAM-1, anti-CD16, anti-HLA-DQ, and anti-CD86 mAbs (BioLegend). The stained cells were analyzed using a FACS Lyric flow cytometer (Becton Dickenson) and the cell population was visualized with FlowJo ver. 10.8.1 (FlowJo LLC) as described in Supplementary Fig. 2.

Results for Supplementary Fig. 5. Expansion with IL-2/IL-18 of NK cells from ATL patients.

(A)Flow cytometric analyses of IL-2/IL-18-mediated expansion of NK cells derived from ATL patients. Four representative flow cytometry diagrams out of 28 ATL patients, ATL-P01–04. The median proportion of $CD56^{+}CD3^{-}$ NK cells after $CD3^{+}$ T cell-depletion was 46.6% (range: 0.45%–87.1%). The proportion of NK cells derived from ATL patients before expansion was comparable to that of HDs. When $CD3^{-}$ PBMC fractions derived from 28 ATL patients were stimulated with IL-2/IL-18 for 10 days, the median proportion of NK cells increased to 92.3% (range: 12.1%–98.5%). The median numbers of NK cells (per mL of blood) before and after expansion were 4.08×10^5 (range: 2.8×10^4–3.52×10^6) and 4×10^6 (range: 4×10^4– 3.6×10^7), respectively. The median expansion rate of NK cells was 11.6-fold (range: 0.1–78.8). Highly purified NK cells were obtained from ATL patients using the IL-2/IL-18 stimulation/expansion system as in the case of HDs. The expansion rate of NK cells from ATL patients was, however, significantly lower than that of HDs ($p = 0.0235$) (Not shown in the figure).

(B) IL-2/IL-18-mediated clustering of NK cells. Microscopic analysis revealed that NK cells derived from ATL patients started to form clusters 4 to 5 days after stimulation with IL-2/IL-18 as in the case of HDs.

(C) Flow cytometric analysis of cell surface markers on IL-2/IL-18-expanded NK cells. On flow cytometric analysis, essentially all the expanded NK cells expressed NKG2D, DNAM-1 and CD16. The median proportions of NKG2D and DNAM-1 in NK cells were 99.01% (range: 91.37%–99.88%) and 93.34% (range: 70.81%–99.19%), respectively. NK cells expressed a high level of CD16; in fact, the median proportion of CD16 in NK cells was 95.08% (range: 70.54%–99.51%). The median proportion of HLA-DQ and CD86 in NK cells was 46.78% (range: 13.57%–81.19%) and 80.38% (range: 52.07%–94.75%), respectively. No significant differences in the expression of NKG2D, DNAM-1, CD16, HLA-DQ, and CD86 were observed between ATL patients and HDs.

Supplementary Note added to Result section 3.5.

Expansion of γδ T cells derived from elderly non-ATL patients. Since most ATL patients are elderly, it is essential to examine the effect of aging on the phenotype and immunological properties of γδ T cells and NK cells to distinguish the effect of the HTLV-1 infection status and age. We obtained peripheral blood samples from 10 elderly non-ATL patients, whose median age was comparable to that of ATL patients.

PMBC derived from 10 elderly non-ATL patients were stimulated/expanded with PTA/IL-2/IL18. The median proportion of γδ T cells in $CD3^+$ lymphocyte fractions before expansion was 0.64% (range: 0.13%–2.52%). None of the elderly non-ATL patients exhibited less than 0.1% of γδ T cells in $CD3^+$ lymphocyte fractions. After expansion of PBMCs with PTA/IL-2/IL-18 for 11 days, the median proportion of γδ T cells in $CD3^+$ lymphocyte fractions increased to 92.90% (range: 72.27%–99.27%). The median numbers of γδ T cells (per mL of blood) before and after expansion were 4×10^3 (range: 4×10^2–3.6×10^4) and 8.5×10^6 (range: 4×10^5–6×10^7), respectively. The median expansion rate of γδ T cells was 2278-fold (range: 180–8089).

On flow cytometric analyses 11 days after stimulation/expansion with PTA/IL-2/IL-18, the median proportions of NKG2D and DNAM-1 in γδ T cells were 97.43% (range: 89.3%–99.89%) and 97.86% (range: 93.5%–99.96%), respectively. γδ T cells expressed CD16 to different degrees; the median proportion of γδ T cells expressing CD16 was 16.27% (range: 1.19%–86.18%). γδ T cells expressed a low level of PD-1 to different degrees, and the median proportion of γδ T cells expressing PD-1 was 15.31% (range: 2.44%–91.2%).

Expansion of NK cells derived from elderly non-ATL patients. $CD3^-$ PBMC derived from elderly non-ATL patients were stimulated with IL-2/IL-18 for 10 days. The median proportion of $CD56^+CD3^-$ NK cell fractions after $CD3^+$ T cell depletion was 40.55% (range: 2.61%–59.8%). After 10 days of incubation, the median proportion of NK cells increased to 93.1% (range: 79.6%–98.5%). The median numbers of NK cells (per mL of blood) before and after expansion were 2.86×10^3 (range: 2.4×10^4–8.48×10^3) and 5×10^6 (range: 6×10^5–1.2×10^7), respectively. The median expansion rate of NK cells was 26.1-fold (range: 1.2–72.5).

On flow cytometric analyses 10 days after IL-2/IL-18 stimulation/expansion, the median proportions of NKG2D and DNAM-1 in γδ T cells were 99.13% (range: 98.35%–99.87%) and 94.34% (range: 85.33%–99.69%), respectively. NK cells expressed a high level of CD16; in fact, the median proportion of NK cells expressing CD16 was 95.52% (range: 85.1%–99.31%). The median proportions of HLA-DQ and CD86 in NK cells were 59.71% (range: 35.29%–86.45%) and 81.55% (range: 46.32%–98.95%), respectively.

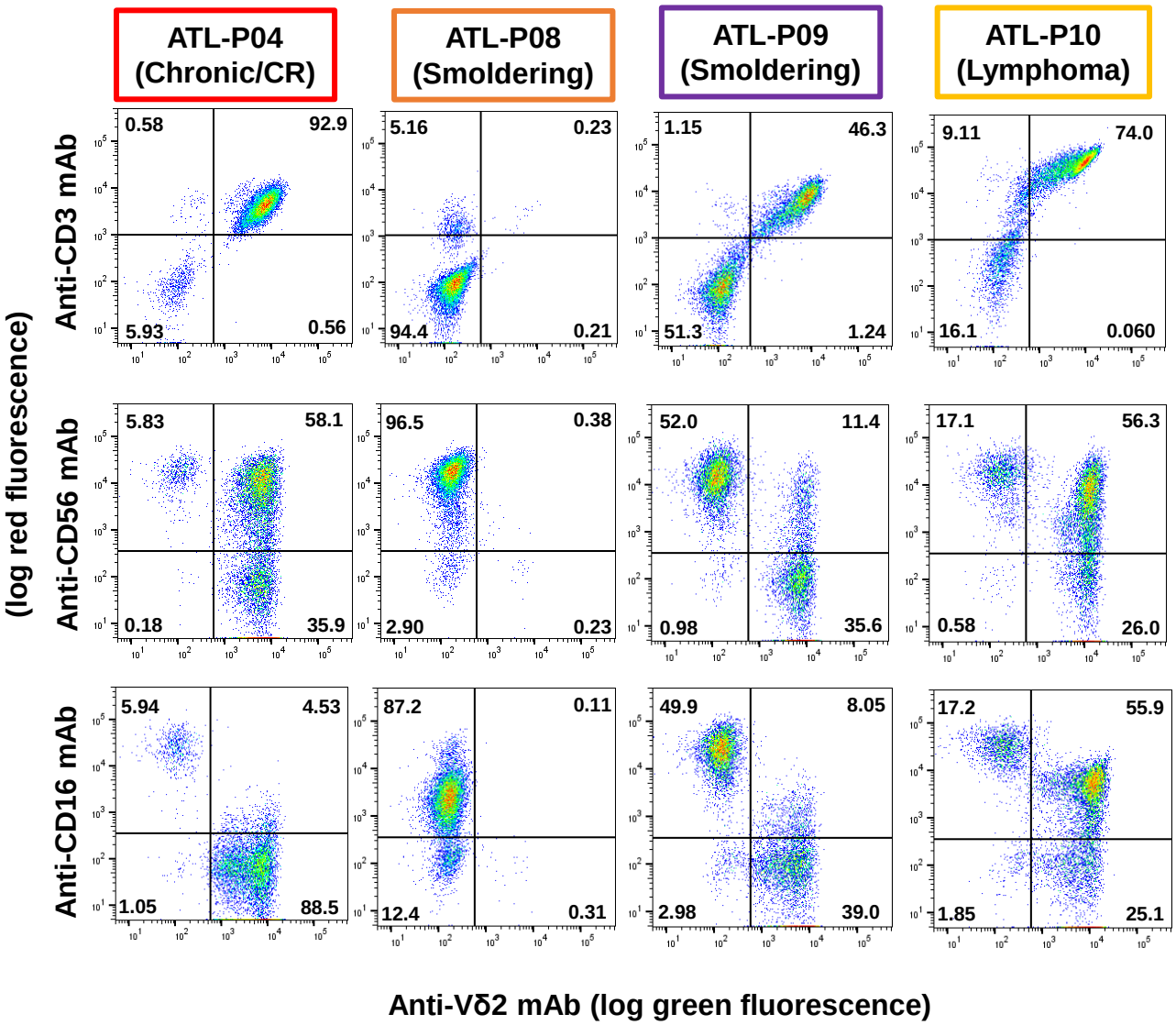

Supplementary Fig. 6. Expansion with PTA/IL-2/IL-18 of γδ T cells and NK cells derived from ATL patients (ATL-P04, 08-14). PBMCs were purified from peripheral blood derived from ATL patients and stimulated/expanded with PTA/IL-2/IL-18, which were stained with PE-conjugated anti-CD3, anti-56 or anti-CD16 mAb and FITC-conjugated anti-Vδ2 mAb, and analyzed through a FACS Lyric flow cytometer.

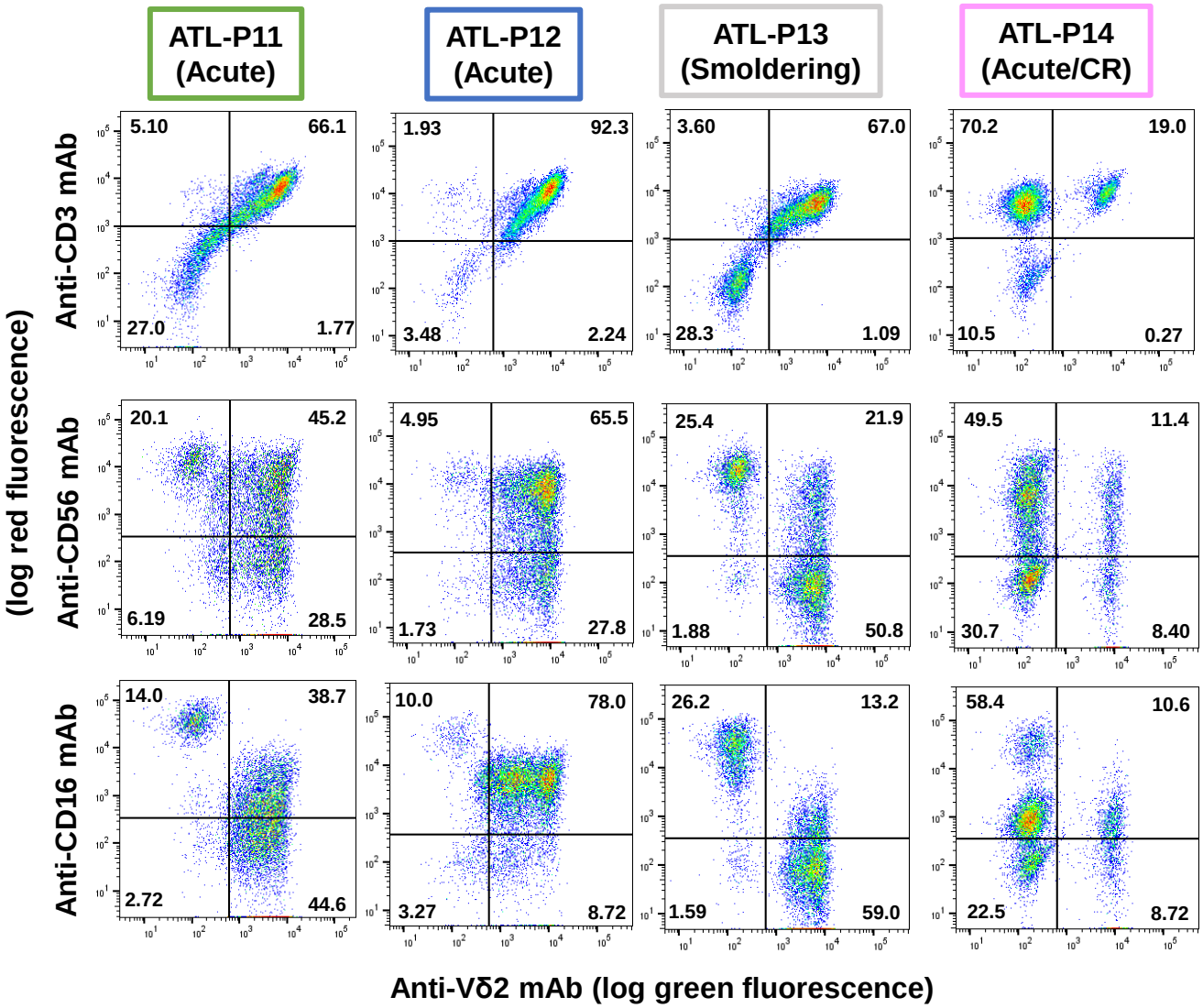

Supplementary Fig. 6. Expansion with PTA/IL-2/IL-18 of γδ T cells and NK cells derived from ATL patients (ATL-P04, 08-14). After stimulation/expansion of PBMCs derived from ATL patients (ATL-P04, 08-14) with PTA/IL-2/IL-18, the cells were stained with PE-conjugated anti-cD3, anti-56 or anti-CD16 mAb and FITC-conjugated anti-Vδ2 mAb, and analyzed through a FACS Lyric flow cytometer.

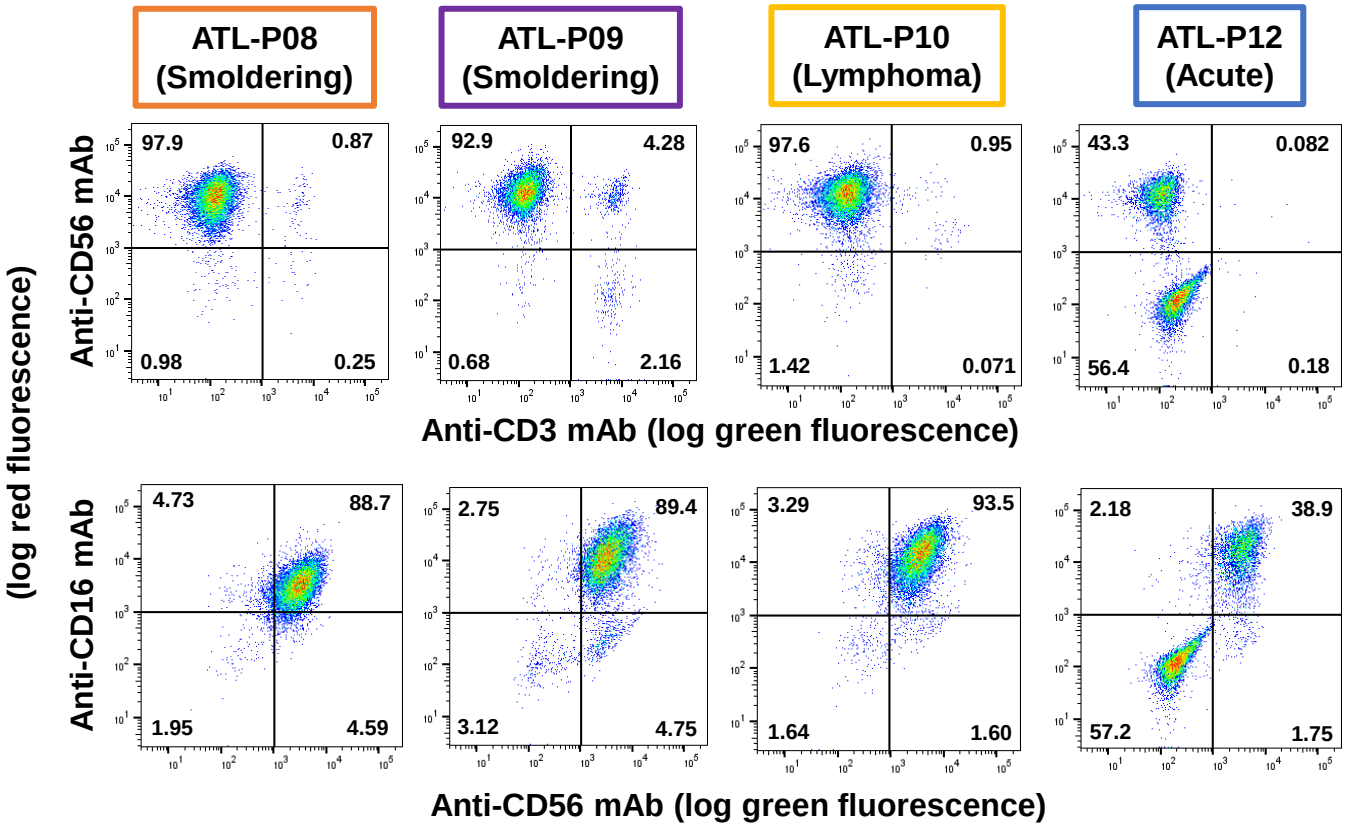

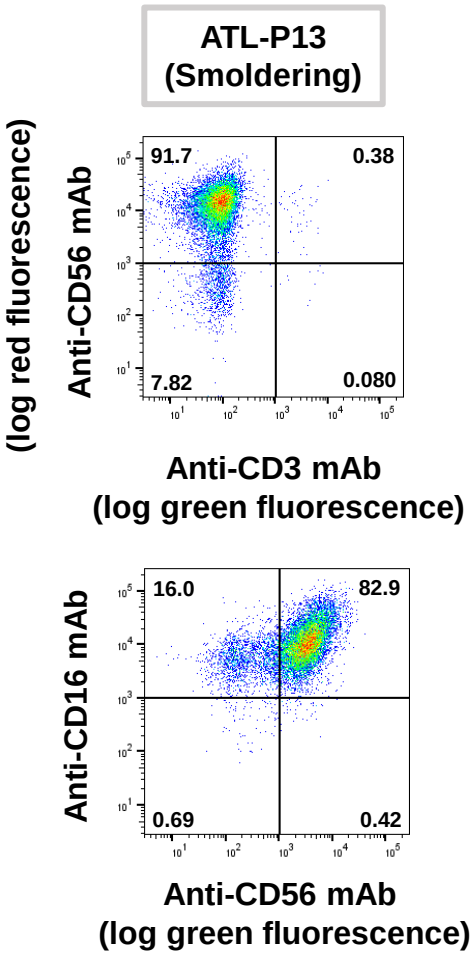

Supplementary Fig. 7. Expansion with IL-2/IL-18 of NK cells derived from ATL patients (ATL-P08-10, 12-13), which were used for the cytotoxicity assay in Fig. 8. PBMCs were purified from peripheral blood derived from ATL patients and stimulated/expanded with IL-2/IL-18, which were stained with PE-conjugated anti-CD56 or anti-CD16 mAb and FITC-conjugated anti-CD3 mAb, and analyzed through a FACS Lyric flow cytometer.

Supplementary Table S1. Summary of flow cytometric analysis, PTA/IL-2-induced expansion of γδ T cells and IL-2/IL-18-induced expansion of NK cells in HDs.

Young, health donors	FACS	PTA/IL-2	PTA/IL-2/IL-18	IL-2/IL-18
HD01	○	○		
HD02	○	○		○
HD03	○	○		
HD04	○	○		
HD05	○			○
HD06	○			○
HD07	○			○
HD08	○	○		
HD09	○	○		
HD10	○	○		
HD11	○			○
HD12	○			○
HD13	○			○
HD14	○	○		○
HD15	○	○		○
HD16	○	○		○

Supplementary Table S2. Summary of the clinical characteristics of 55 ATL patients. ATL, adult T-cell leukemia–lymphoma; mogamulizumab, defucosylated anti-CCR4 monoclonal antibody; PSL, prednisolone; bexarotene, retinoid X receptor (RXR) agonist; lenalidomide, potent inhibitor of TNF-α; sIL-2R, soluble interleukin-2 receptor; LDH, lactate dehydrogenase; Alb, albumin; BUN, blood urea nitrogen; Ca, calcium; corrected Ca = serum Ca + 0.8*(normal albumin - patient albumin); WBCs, white blood cells; Ly, lymphocyte; Ab-Ly, abnormal lymphocyte; IQR, interquartile range.

Characteristic	n = 55
Male sex, n (%)	29 (52.7)
Age at blood sampling, y, median (min, max, IQR)	72 (34, 86, 63.5-78)
Shimoyama classification at diagnosis, n (%)	
Smoldering subtype	13 (23.6)
Favorable chronic subtype	9 (16.4)
Unfavorable chronic subtype	5 (9.1)
Lymphoma subtype	4 (7.3)
Acute subtype	24 (43.6)
Performance status (PS)	1 (0, 4, 0-1)
Previous treatments at the time of blood sampling, n (%)	
Untreated (with no anticancer drugs)	31 (56.4)
Undergoing anticancer drug treatment	10 (18.2)
Post anticancer drug treatment	14 (25.5)
Breakdown of anticancer drug treatment, n (%)	
Only chemotherapy	12 (21.8)
Only mogamulizumab	1 (1.8)
Chemotherapy + mogamulizumab	7 (12.7)
Chemotherapy + lenalidomide	1 (1.8)
Bexarotene	3 (5.5)
Use of PSL or immunosuppressants at the time of blood sampling	
PSL	6 (10.9)
Immunosuppressants	1 (1.8)
Laboratory examinations, median (min, max, IQR)	
sIL-2R (U/ml)	969 (60, 100000, 634.5-4379)
LDH (IU/L)	214 (94, 3882, 72-266)
Alb (g/dL)	4.1 (2.1, 4.7, 3.8-4.3)
BUN (mg/dL)	16 (7, 37, 13-20)
Corrected Ca (mg/dL)	9.5 (8.7, 11, 9.2-9.7)
WBCs ($\times 10^9$/L)	6.6 (2.8, 202.4, 4.825-10.15)
Ly (%)	28 (0, 84, 13-39)
Ab-Ly (%)	3 (0, 96, 0-12)

Supplementary Table S3. The Shimoyama classification at the first diagnosis and the outcome at the time of blood sampling. CR, complete response; PR, partial response.

Shimoyama Classification at Diagnosis	Patients Who Underwent Blood Sampling	Patients who Achieved CR	Patients who Achieved PR
Smoldering subtype (n=13)	3	0	3
Favorable chronic subtype (n=9)	3	2	0
Unfavorable chronic subtype (n=5)	1	0	0
Lymphoma subtype (n=4)	2	2	0
Acute subtype (n=24)	15	9	3

A total of 55 ATL patients (29 males and 26 females) in the Departments of Hematology and Dermatology of Nagasaki University Hospital were enrolled in this study between April 2013 and January 2023. We selected patients with a definitive diagnosis of ATL at the Department of Hematology before blood sampling, using evidence of the monoclonal integration of HTLV-1 proviral DNA and clinical and laboratory findings. Patient information was retrospectively collected, beginning at the time the blood sampling was conducted. Clinical characteristics of 55 ATL patients are summarized in Supplementary Table 2. The median age at the time of blood sampling was 72 years (range: 34 – 86 years). The most common subtype of ATL at first diagnosis, based on the Shimoyama classification [8], was the acute subtype (43.6%). Patients who underwent hematopoietic stem cell transplantation were excluded. The Shimoyama classification at the first diagnosis and the outcome at the time of the blood sampling are summarized in Table 2. Among the ATL patients enrolled, 31 (56.4%) had not received any anticancer drugs, and 24 (43.6%) had a history of anticancer drug use at the time of blood collection. Of these, 6 patients were undergoing chemotherapy treatment and 4 patients were taking lenalidomide or bexarotene internally. At the same time, the following laboratory tests were conducted, all of which were previously established biomarkers for aggressive subtype factors of ATL: levels of serum soluble interleukin-2 receptor (sIL-2R) (U/mL), lactate dehydrogenase (LDH, IU/L), albumin (Alb. g/dL), blood urea nitrogen (BUN, mg/dL), corrected calcium (Ca, mg/dL), white blood cells (WBCs $\times 10^9$/L), lymphocyte (Ly, %), and abnormal lymphocytes (Ab-Ly, %),.

ATL's onset requires a long latency period of approximately 50 – 60 years after infection with HTLV-1 in infants, and ATL, thus, occurs mostly in elderly HTLV-1-infected individuals. Aging is reported to result in the remodeling of T-cell immunity and to be associated with poor clinical outcomes in age-related diseases [61]. In addition, the immune system is also reported to be suppressed in ATL patients [24-26]. It is, therefore, a prerequisite to examine the immunological properties of γδ T cells and NK cells from ATL patients and the effects of aging and immunosuppression status associated with HTLV-1 infections on the effector functions of innate immune cells. To examine the effect of aging on γδ T-cell populations in PBMCs, 10 elderly non-ATL patients (8 males and 2 females) were enrolled in this study; who suffered from epidermal cyst, atopic dermatitis, skin ulcer, alopecia, angioleiomyoma, post-herpes zoster, and prurigo.

Supplementary Table S4. Summary of flow cytometric analysis, PTA/IL-2-induced expansion of γδ T cells, PTA/IL-2/IL-18-induced expansion of γδ T cells and IL-2/IL-18-induced expansion of NK cells in ATL patients.

ATL Patient	FACS	PTA/ IL-2	PTA/ IL-2/IL-18	IL-2/ IL-18	ATL Patient	FACS	PTA/ IL-2	PTA/ IL-2/IL-18	IL-2/ IL-18
ATL-P01	○		○	○	ATL-P29	○		○	○
ATL-P02	○		○	○	ATL-P30	○		○	○
ATL-P03	○		○	○	ATL-P31	○	○	○	
ATL-P04	○		○	○	ATL-P32	○	○	○	
ATL-P05	○		excluded	○	ATL-P33	○	○	○	
ATL-P06	○		○	○	ATL-P34	○	○	○	
ATL-P07	○		○	○	ATL-P35	○	○	○	
ATL-P08	○		○	○	ATL-P36	○	○	○	
ATL-P09	○		○	○	ATL-P37	○	○	○	
ATL-P10	○		○	○	ATL-P38	○	○	○	
ATL-P11	○		○	○	ATL-P39	○	○	○	
ATL-P12	○		○	○	ATL-P40	○	○	○	
ATL-P13	○		○	○	ATL-P41	○	○	○	
ATL-P14	○		○	○	ATL-P42	○	○	○	
ATL-P15	○		○	○	ATL-P43	○	○	○	
ATL-P16	○		excluded	○	ATL-P44	○	○	○	
ATL-P17	○		○	○	ATL-P45	○	○	○	
ATL-P18	○		○	○	ATL-P46	○	○	○	
ATL-P19	○		○	○	ATL-P47	○	○	○	
ATL-P20	○		○	○	ATL-P48	○	○	○	
ATL-P21	○		○	○	ATL-P49	○	○	○	
ATL-P22	○		○	○	ATL-P50	○	○	○	
ATL-P23	○		○	○	ATL-P51	○	○	○	
ATL-P24	○		○	○	ATL-P52	○	○	○	
ATL-P25	○		○	○	ATL-P53	○	○	○	
ATL-P26	○		○	○	ATL-P54	○	○	○	
ATL-P27	○		○	○	ATL-P55	○	○	○	
ATL-P28	○		○	○					

Supplementary Table S5. Summary of flow cytometric analysis, PTA/IL-2/IL-18-induced expansion of γδ T cells and IL-2/IL-18-induced expansion of NK cells in elderly non-ATL patients.

Elderly non-ATL patients	FACS	PTA/IL-2	PTA/IL-2/IL-18	IL-2/IL-18
Elderly-P01	○		○	○
Elderly-P02	○		○	○
Elderly-P03	○		○	○
Elderly-P04	○		○	○
Elderly-P05	○		○	○
Elderly-P06	○		○	○
Elderly-P07	○		○	○
Elderly-P08	○		○	○
Elderly-P09	○		○	○
Elderly-P10	○		○	○